Biogeosystem Technique

Issued since 2014.

E-ISSN 2413-7316
2024. 11(2). Issued 2 times a year

Journal is indexed by: **Cross Ref** (USA), **Electronic scientific library** (Russia), **MIAR** (Spain), **Open Academic Journals Index** (USA), **CiteFactor – Directory of International Reseach Journals** (Canada).

All manuscripts are peer reviewed by experts in the respective field. Authors of the manuscripts bear responsibility for their content, credibility and reliability.

Editorial board doesn't expect the manuscripts' authors to always agree with its opinion.

Postal Address: 1717 N Street NW, Suite 1, Washington, District of Columbia 20036

Website: https://bgt.cherkasgu.press
E-mail: kalinitch@mail.ru

Founder and Editor: Cherkas Global University

Release date 25.12.2024
Format 21 × 29,7/4.

Headset Georgia.

Order № B-26.

Biogeosystem Technique

2024

Is. 2

Articles

In Memoriam

Published in the USA
Biogeosystem Technique
Issued since 2014.
E-ISSN: 2413-7316
2024. 11(2): 84-90

DOI: 10.13187/bgt.2024.2.84
https://bgt.cherkasgu.press

Articles

Cation Exchange Capacity in the Arid Soils of the Republic of Kalmykia

Raisa A. Mukabenova [a], Altana B. Adyanova [a], Anatoly V. Barakhov [b], Alexey A. Buluktaev [a], Saglara S. Mandzhieva [a, b, *], Arpna Kumari [c], Rupesh K. Singh [d], Avnish Chauhan [e]

[a] Kalmyk Scientific Center of the Russian Academy of Sciences, Elista, Russian Federation
[b] Southern Federal University, Rostov-on-Don, Russian Federation
[c] University of Tokyo, Tokyo, Japan
[d] University of Minho, Braga, Portugal
[e] Graphic Era Hill University, Bharu Wala Grant, Uttarakhand, India

Paper Review Summary:
Received: 2024, November 19
Received in revised form: 2024, December 13
Acceptance: 2024, December 26

Abstract

On the basis of field research, the current state of soils in the eastern zone of the Republic of Kalmykia was studied. The predominant soil cover in this area is represented by brown saline soils and brown-desert soils in a complex with salt licks. The purpose of the study is to study the absorption complex, as well as the composition and content of exchangeable cations in the soils of the eastern zone of the Republic of Kalmykia. cations: calcium (Ca^{2+}) and magnesium (Mg^{2+}) and an assessment of the level of soil absorption capacity in 7 settlements of the Yashkul district of the Republic of Kalmykia. To conduct the research, 15 monitoring sites were placed on the borders and in the center of settlements, the background sample was taken at a distance of 500 m from the boundaries of the residential zone. The determination of the physical and chemical properties of the soils was carried out according to GOST and generally accepted methods. The results of the study showed that the level of absorption capacity of soils in the study area ranges from low to medium. The absorbent complex is saturated with the cations Ca^{2+} and $Mg^{2+,}$ and the content of exchangeable Ca^{2+} predominates over the content of Mg^{2+} in the range of 2 to 4 times.

Keywords: Republic of Kalmykia, solonets, chemical properties of soils, exchangeable cations, soil absorption complex.

1. Introduction

To date, much attention has been paid to the study of exchangeable cations, as they affect the chemical, physical and biological properties of soils, are easily absorbed by the root system of plants and are an important source of mineral nutrition (Giedroyc, 1933; Karpachevsky et al.,

[*] Corresponding author
E-mail addresses: msaglara@mail.ru (S.S. Mandzhieva)

2007). The founder of the first studies on soil absorption capacity, K.K. Giedroyc (1975), who was the first to introduce the term soil absorption complex and used the term soil absorption capacity as the sum of all exchangeable cations, which can be displaced from the soil, argued that the best fertility is possessed by soils saturated with potassium and magnesium (Pinsky, 1990). The amount of magnesium absorbed should be 20-40% of the calcium absorbed (Antipova-Karataeva, Antipov-Karataev, 1940). In the soils of arid regions, such as the Republic of Kalmykia, the most important factor for diagnosing the processes of soil formation and soil fertility are the exchangeable cations of the soil absorption complex Ca^{2+}, Mg^{2+}.

Calcium is present exclusively in all soils, but in different amounts and in different ratios with other cations. It makes the soil structure loose, acts as a binder between clay and organic matter (Kershberger, Proysker, 2007). Magnesium is a concomitant element (companion) of potassium, often found in soils in the ratio of Ca^{2+} cations: Mg^{2+}=5:1, but when this ratio shifts towards Mg^{2+}, there is an increase in the alkalinity of soils due to the presence of magnesium carbonates and bicarbonates in the soil environment (Vorobyeva, Pankova, 1995; Vorobyova 2006; Okorkov, 1994). The well-known scientist G.D. Unkanzhinov et al. (2005) devoted his scientific work to the study of the dynamics of exchangeable potassium content in the soils of the Republic of Kalmykia for 1966-2013. The dynamics, based on agrochemical studies over the past 50 years, shows that the weighted average content of exchangeable potassium in the soils of arable land in the republic is at the high availability level, but there is a negative balance of this element. The monograph "Red Book of Soils and Ecosystems of Kalmykia" (Unkanzhinov et al., 2005; Okorkov, 1994) provides values of absorption capacity and composition of exchangeable cations in a number of main types of soils: solonetz, meadow-brown, light chestnut solonetz, meadow-chestnut, chestnut solonetz, chernozem, which are characteristic soils of protected natural areas of Kalmykia. Considering valuable soil and biological objects in the system of specially protected areas of the Republic of Kalmykia, (Tashninova, 2000) indicated that these objects are confined to the main natural-territorial formations. In general, modern data on the composition of exchangeable cations in the soils of the Republic of Kalmykia have not been studied sufficiently, which determines the relevance of this topic. The purpose of the study was to study the absorption complex, as well as the composition and content of exchangeable cations in the soils of the eastern zone of the Republic of Kalmykia.

2. Materials and methods

During the 2020 seasonal expedition in the Yashkul district, materials were selected based on data on the physical and chemical composition of the soils. 7 settlements in the Yashkul district were chosen as the subject of the study: Chilgir village, Ulan-Erge village, Elvg village, Ermeli village, Khogn village, Gashun village, Yashkul village (Figure 1).

Fig. 1. Sampling sites in the Yashkul district of the Republic of Kalmykia

The basis of the soil cover of this territory is a zonal group of brown saline soils and brown desert-steppe saline soils in combination with saline soils.

The structural composition of the study area is represented by brown semi-desert soils, with feather-grass-fescue, wormwood-feather grass vegetation characteristic of them. Information about the natural conditions and characteristics of this area was studied in detail in the work of A.B. Adyanova et al. (2023). The physicochemical characteristics of soils were studied using generally accepted methods: the pH of an aqueous suspension was determined by the potentiometric method with a hydrogen electrode (GOST, 2011) organic matter according to Tyurin modified by V.N. Simakov (GOST, 1993) exchange cations Ca^{+2} and Mg^{+2} according to GOST 26487-85 (GOST, 1985) trilonometrically. The level of absorption capacity was assessed using the scale given in Table 1 (Remezov, 1957).

Table 1. Assessment of the level of cation exchange capacity (CEC)

CEC	mEq/100 g soil
Low	<10
Average	10-20
High	20-40
Very high	>40

Processing of the data obtained was carried out using descriptive statistics in the Statistica v.12 program.

3. Results and discussion

In the course of studies on the extraction of water from soils in the Yashkul district of the Republic of Kalmykia, indicators such as organic carbon content, environmental reaction (pH), exchangeable cations Ca^{2+} and Mg^{2+}, as well as CEC were studied (Figures 2–7).

As a result of the work carried out, it was found that in the soils of the study area, the organic carbon in the surface layer (0–20 cm) is in the range of 0.31–1.86%, which indicates a very low content (Figure 2).

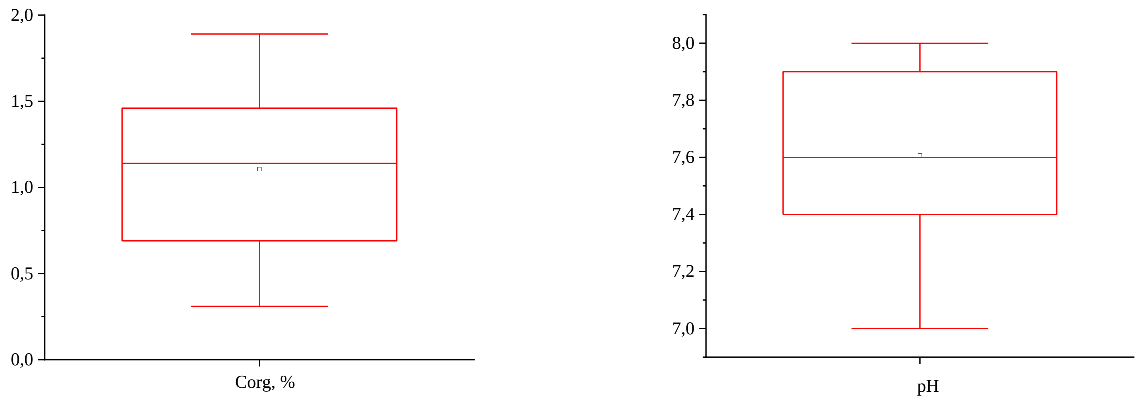

Fig. 2. Organic carbon content, %, pH in soils of the Yashkul district of the Republic of Kalmykia

The pH response of the soil environment varies from 7.0 to 8.0, which corresponds to a neutral and slightly alkaline reaction (Figure 2). The content of exchangeable cations Ca^{2+} ranges from 0.25 to 19.77 mmol(mg-eq)/100 g soil (very low to low), and for Mg^{2+} from 8.67 to 55.43 mmol(mg-eq)/100 g soil (increased to very high), it can also be concluded that the content of exchangeable calcium prevails over the exchangeable magnesium in the limit from 2 to 4 times (Figure 3).

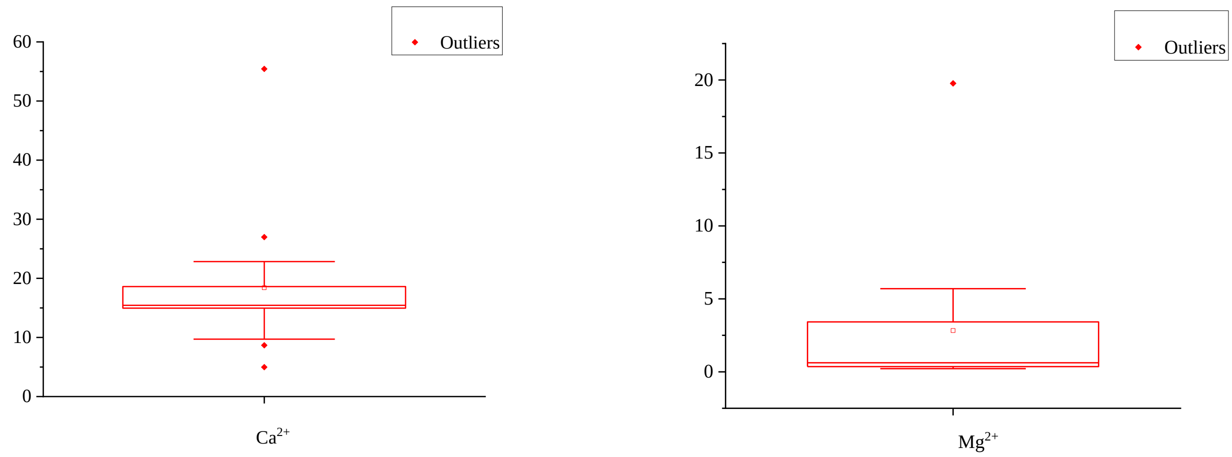

Fig. 3. Exchangeable cations Ca^{2+}, Mg^{2+} mmol (mg-eq)/100 g soil of the Yashkul district of the Republic of Kalmykia

According to the scale for assessing the level of soil absorption capacity, the CEC is in the range of 5.2–75.2 mmol (mEq)/100 g soil, indicating a variation of this indicator from low to very high, but most of the soils studied are in the medium range (Figure 4). Minimum values: pH, Corg, Ca^{2+}, Mg^{2+}, CEC are found mainly at the background sites, and this pattern is true for most of the sites studied (Figures 5–7).

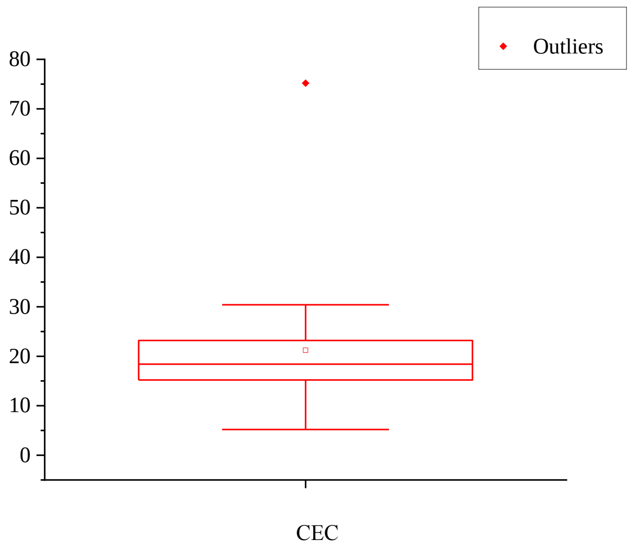

Fig. 4. CEC mmol (mg-eq)/100 g soil of the Yashkul district of the Republic of Kalmykia

Chilgir, Ermeli and Yashkul soil cover of is represented by brown desert-steppe saline soils in combination with saline soils, the pH of the soil solution varies from neutral to slightly alkaline (7.2–7.7) in terms of organic carbon content, this area varies from low-humus and medium-humus (0.31–1.89%), the saturation with exchangeable cations also varies in Mg^{2+} from very high to very low (0.56–19.77) mmol(mg-eq)/100 g soil, Ca^{2+} – changed to very low (8.67–55.43) mmol (mg-eq)/100 g, and in terms of CEC capacity there is also a variation from very high to low (10.4–75.2) mmol(mg-eq)/100 g soil (Figures 5, 6). The highest values in these settlements were found in the Yashkul settlement – for the exchange cations Mg^{2+} – 19.77 mmol(mg-eq)/100 g soil, Ca^{2+} – 55.43 mmol (mg-eq)/100 g soil and CEC – 7.52 mmol (mg-eq)/100 g soil (edge of the settlement) (Figures 3–4), and according to the pH 7.7 and Corg indices of 1.68% (background sample) (Figures 5–7).

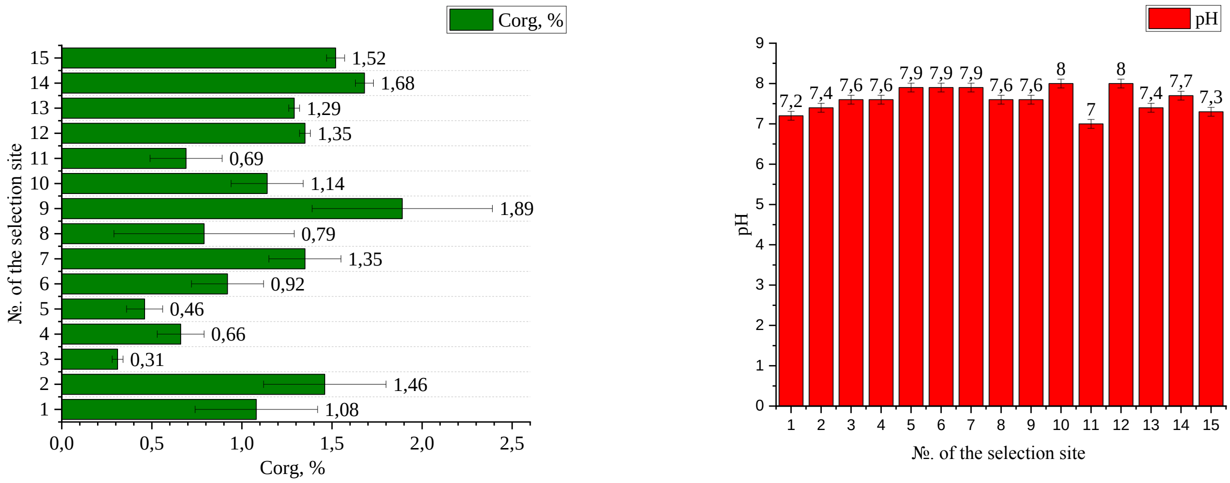

Fig. 5. Organic carbon content and pH in soils of the Yashkul district of the Republic of Kalmykia

On the territory of the villages of Khogn and the village of Gashun, brown saline soils prevail with saline soils, the reaction of the pH of the soil solution changes from neutral to alkaline (7.0 to 8.0), the variation of organic carbon within (0.69 %–1.35 %) low-humus and medium-humus soils, exchangeable cations and for Mg^{2+} 0.29–3.01 mmol (mg-eq)/100 g soil and for Ca^{2+} 9.71–22.84 mmol(mEq)/100 g soil ranges from very low to medium, with CEC within the medium to high range of 10.0–23.2 mmol(mEq)/100 g soil (Figures 5–7).

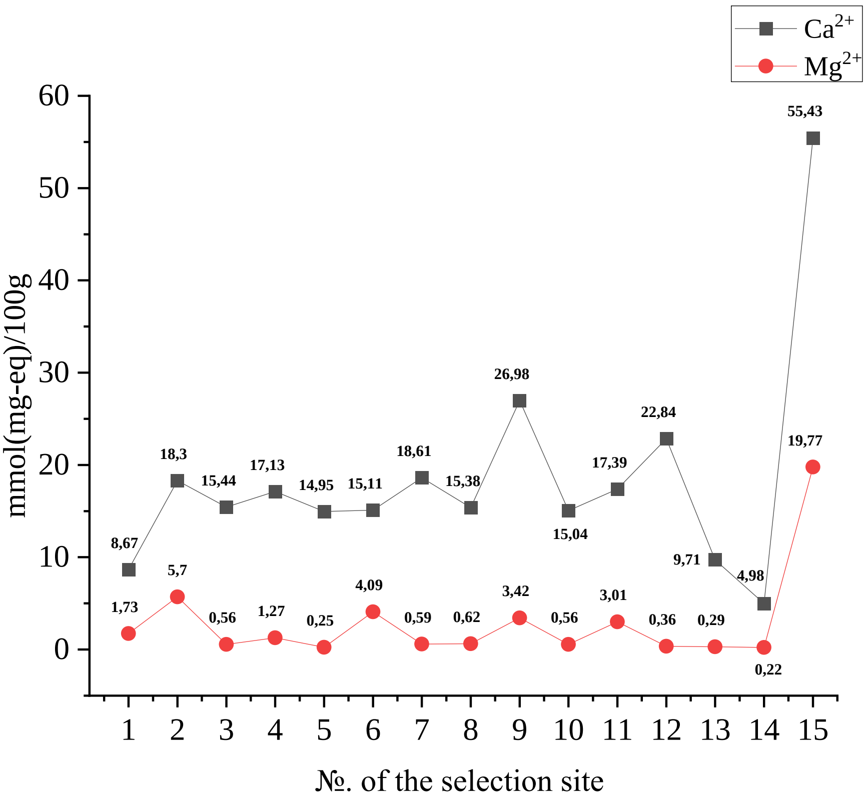

Fig. 6. Exchange cations Ca^{2+}, Mg^{2+} in the soils of the Yashkul District of the Republic of Kalmykia

The highest indicators values of were found in the village of Hogn (background) for the exchange cation Mg^{2+} 3.01 mmol (mg-eq)/100 g soil – very low (Figure 6), and in the center of the settlement the pH 8.0 alkaline and organic carbon increased (1.14%). In the village of Gashun, the values for Ca^{2+} 22.84 mmol (mg-eq)/100 g soil – average saturation and CEC 23.2 mmol (mg-eq)/100 g soil high level increased (Figure 7). The main type of soil in the village of Evlg is meadow solonets, the pH of the soil solution is slightly alkaline (7.9), in terms of organic carbon, low-humus soil – 1.35 % (Figure 5), Mg^{2+} – 0.59 mmol (mg-eq)/100 g soil (very low), Ca^{2+} – 18.61 mmol (mg-eq)/100 g soil (low) in saturation with exchange bases, CEC – 19.2 mmol (mg-eq)/100 g soil average (Figures 5–7).

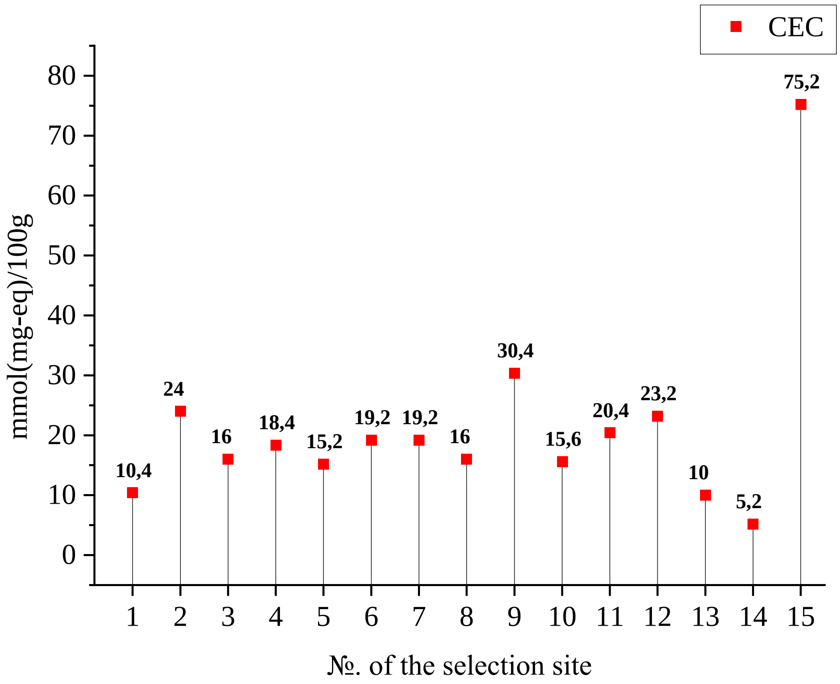

Fig. 7. Exchange cations Ca^{2+}, Mg^{2+}, CEC in the soils of the Yashkul District of the Republic of Kalmykia

The village of Ulan-Erge is represented by brown saline and saline soils, the pH of the soil solution is slightly alkaline 7.6–7.9, organic carbon is 0.46–0.92% (slightly humus to low-humus) (Figure 5), exchangeable cations at Mg^{2+} 0.25–4.09 mmol (mg-eq)/100 g soil are very low and at Ca^{2+} 14.95–17.13 mmol(mg-eq)/100 g soil low saturation, and CEC is in the range of 15.2–19.2 mmol (mg-eq)/100 g soil medium level absorption capacity (Figure 7).

4. Conclusion

Studies carried out in the Yashkul district have shown that this territory is mainly represented by a group of brown-saline to brown-semi-desert soils, which are typical for this territory. Chemical analysis of water extracts indicates that soils have a low organic carbon content (less than 2 %), which indicates low humus and low soil fertility, the pH in a larger mass of horizons (0–20 cm) is slightly alkaline (pH from 7–8 units). The saturation of the absorbing complex of metabolic Ca^{2+} and Mg^{2+}, as well as the predominance of calcium over magnesium. The content of exchange cations Ca^{2+} ranges from 0.25 to 19.77 mmol(mg-eq)/100 g soil (very low to low), and for Mg^{2+} from 8.67 to 55.43 mmol(mg-eq)/100 g soil (increased to very high). The absorption capacity of the studied soils varies from low to medium. The data obtained during the survey confirm the favorability of cultivation and cultivation of agricultural crops in the territory of the Yashkul district of the Republic of Kalmykia as an area belonging to the zone of risky farming and the correspondence exists of indicators of soil characteristics in the territory of the Republic of Kalmykia.

5. Conflict of interest information

The authors declare that there is no conflict of interest.

6. Acknowledgements

The article was prepared within the framework of the state subsidy "Asymmetrically developing territories in the face of traditional and new challenges: a study of the dynamics of socioeconomic processes and the variability of the environmental situation" (state registration number of research, development and technological work for civil purposes (hereinafter referred to as R&D): 122022700133-9).

References

Adyanova et al., 2023 – *Adyanova, A., Buluktaev, A., Mukabenova, R., Mandzhieva, S., Rajput, V., Sayanov, V., Djimbeev, N., Sushkova, S.* (2023). Characterization of arid soil quality: Physical and chemical parameters. *Eurasian J. Soil Sci.* 12(2): 151-158.

Antipova-Karataeva, Antipov-Karataev, 1940 – *Antipova-Karataeva, T.F., Antipov-Karataev, I.N.* (1940). On the question of determining the constants of cation exchange in soils. *Soil Science.* 2: 52-55.

Giedroyc, 1975 – *Giedroyc, K.K.* (1975). Selected works. *Nauka*. 639.

Giedroyc, 1993 – *Giedroyc, K.K.* (1993). The doctrine of the absorption capacity of soils. *Selkhozgiz*, 203.

GOST 26213-91, 1993 – Interstate standardization system. GOST 26213-91. Soils. Methods for the determination of organic matter. 1993. [Electronic resource]. URL: https://files.stroyinf.ru/Data2/1/4294828/4294828267.htm

GOST 26483-85, 1985 – Interstate standardization system. GOST 26483-85. Soils. Preparation of salt extract and determination of its pH by the TSINAO method. 1985. [Electronic resource]. URL: https://docs.cntd.ru/document/1200023490

GOST 26487-85, 1985 – Interstate standardization system. GOST 26487-85. Soils. Preparation of salt extract and determination of its pH, determination of exchangeable calcium and exchangeable (mobile) magnesium by TSINAO methods (as amended). Moscow: Publishing House of Standards, 1985. 20.

Karpachevsky et al., 2007 – *Karpachevsky, L.O., Zubkova, T.A., Tashninova, L.N., Rudenko, R.N.* (2007). Soil cover and parcel structure of forest biogeocenosis. *Forestry* (6): 107-113.

Kershberger, Proysker, 2007 – *Kershberger, M., Proysker, T.* (2007). Nitrogen is important for the soil. And the calcium? *New agriculture*. 4: 68-70.

Okorkov, 1994 – *Okorkov, V.V.* (1994). Solonets and their colloidal chemical nature. *Catalog of documents from 1831 to the present*. 240.

Pinsky, 1990 – *Pinsky, D.L.* (1990). Ion-exchange absorption of magnesium by soils. *Agrochemistry*. 2: 81-90.

Remezov, 1957 – *Remezov, N.P.* (1957). Soil colloids and the absorption capacity of soils. State Publishing house of agricultural literature. 234.

Tashninova, 2000 – *Tashninova, L.N.* (2000). The Red Book of Soils and ecosystems of Kalmykia. *Elista: APP "Dzhangar"*. 216.

Unkanzhinov, et al., 2005 – *Unkanzhinov, G.D. Badmaeva, Z.B., Nemkeeva, V.V.* (2005). Dynamics of the content of exchangeable potassium in the soils of arable land of the Republic of Kalmykia. *Fertility*. 3: 21-23.

Vorobyeva, Pankova, 1995 – *Vorobyeva, L.A., Pankova, E.I.* (1995). The nature of alkalinity and diagnostics of alkaline soils of arid and semiarid territories. *Soil Science*. 1: 108-110.

Vorobyova, 2006 – *Vorobyova, L.A.* (2006). Theory and practice of chemical analysis of soils. *GEOS*. 400.

Published in the USA
Biogeosystem Technique
Issued since 2014.
E-ISSN: 2413-7316
2024. 11(2): 91-107

DOI: 10.13187/bgt.2024.2.91
https://bgt.cherkasgu.press

Advancements in Crystallogens Nanoparticles Fabricated by Agricultural Wastes

Prachi Kurhade [a, *], Himanshu Bansal [a], Priyadarshani Rajput [b], Sakshi Singh [c]

[a] Indian Institute of Science Education and Research Tirupati, Jangalapalli Andhra Pradesh, India
[b] Academy of Biology and Biotechnology, Southern Federal University, Rostov-on-Don, Russian Federation
[c] Faculty of Biology, Yerevan State University, Yerevan, Armenia

Paper Review Summary:
Received: 2024, November 10
Received in revised form: 2024, December 8
Acceptance: 2024, December 26

Abstract

Using nanotechnology in agriculture has become a game-changing strategy to improve soil health, crop yield, and sustainability. This article investigates the production and uses of several nanoparticles obtained from agricultural wastes, such as those based on carbon, silicon, and lead. Carbon nanoparticles are created by processes such chemical vapor deposition, pyrolysis, and hydrothermal synthesis. They are valued for their large surface area, mechanical strength, and electrical conductivity. The nutrient cycle, water retention, and soil structure are all markedly enhanced by these nanoparticles. Synthesized from plentiful agricultural leftovers, silicon nanoparticles offer an affordable means of creating green fertilizers and boosting plant growth. Many studies have been done on their synthesis using chemical, physical, and environmentally friendly approaches. This article highlights the potential and challenges of utilizing nanotechnology in agriculture, emphasizing the importance of sustainable synthesis methods. The development of efficient nanoparticle production techniques from agricultural wastes offers innovative solutions to agricultural challenges, promoting a sustainable and resilient agricultural system.

Keywords: Nanomedicine, sustainable solutions, waste management

1. Introduction

Agricultural wastes are defined as the leftover plant residues that remain after the primary crop has been harvested. These wastes include a variety of materials such as leaves, stems, husks, roots, branches, and other organic components that are discarded or not used directly in the production process.

Globally, the accumulation of such waste is significant, with agricultural by-products forming one of the largest sources of organic waste. For instance, in the European Union alone, around 700 million tons of agricultural waste are generated annually, reflecting a considerable environmental challenge (Yearbook, 2013; Fritsch et al., 2017; Wikipedia contributors…, 2024; Mohite et al., 2022).

[*] Corresponding author
E-mail addresses: himanshubansal211125@students.iisertirupati.ac.in (P. Kurhade)

In recent years, nanotechnology has emerged as a powerful tool for addressing environmental and waste management challenges. Nanotechnology refers to the manipulation of materials at the atomic or molecular scale, typically below 100 nanometers, leading to the creation of nanoparticles. These particles possess unique properties such as enhanced chemical reactivity, increased surface area, and novel optical or electrical behaviors. The integration of nanotechnology with green chemistry has opened new avenues for environmentally friendly agricultural waste management. Green chemistry emphasizes the design of chemical processes that minimize the use and generation of hazardous substances, making it a key player in sustainable waste recycling (Madhumitha, 2013).

Agricultural waste, or agro-waste, is composed of a variety of organic substances, mainly cellulose, hemicellulose, and lignin. In addition, some waste may contain proteins, oils, and other bioactive compounds. Agro-processing wastes include the remains of crops like rice, wheat, sugarcane, corn, and vegetables. For example, rice bran, which is a by-product of rice milling, has been extensively studied as a potential source for bioethanol production. Beyond plant waste, livestock waste, including animal manure such as cow dung, also constitutes a significant portion of agricultural waste. These organic residues are rich in essential nutrients and carbon, making them valuable for recycling into biofuels, fertilizers, and more recently, for use in the production of nanoparticles.

This review focuses on the utilization of agricultural waste in the synthesis of nanoparticles, particularly crystallogen-based nanoparticles. Crystallogens are elements from Group 14 of the periodic table, comprising carbon, silicon, germanium, tin, and lead. These elements exhibit versatile chemical behaviors, making them ideal candidates for nanoparticle synthesis. Nanoparticles of crystallogens have attracted considerable attention for their diverse applications, ranging from medicine to environ-mental remediation. For instance, carbon-based nanoparticles, such as carbon-coated metals, are extensively used in catalysis and energy storage. Silicon nanoparticles (SiNPs), on the other hand, are employed in the semiconductor industry and for biomedical imaging. In this review, we will explore the green synthesis methods used to produce these nanoparticles and their applications in various fields, including agriculture, medicine, and environmental monitoring. Nanoparticles synthesized from agro-waste present a dual benefit: reducing environmental pollution caused by waste accumulation and providing a sustainable source of nanomaterials. Moreover, metals like silver, gold, and zinc are used in combination with agro-waste to create nanoparticles that exhibit strong antimicrobial properties, enhancing their potential use in fields such as medicine, agriculture (as pesticides), and environmental monitoring. This integration of waste management and nanotechnology offers an innovative approach to addressing some of the most pressing global challenges (Figure 1).

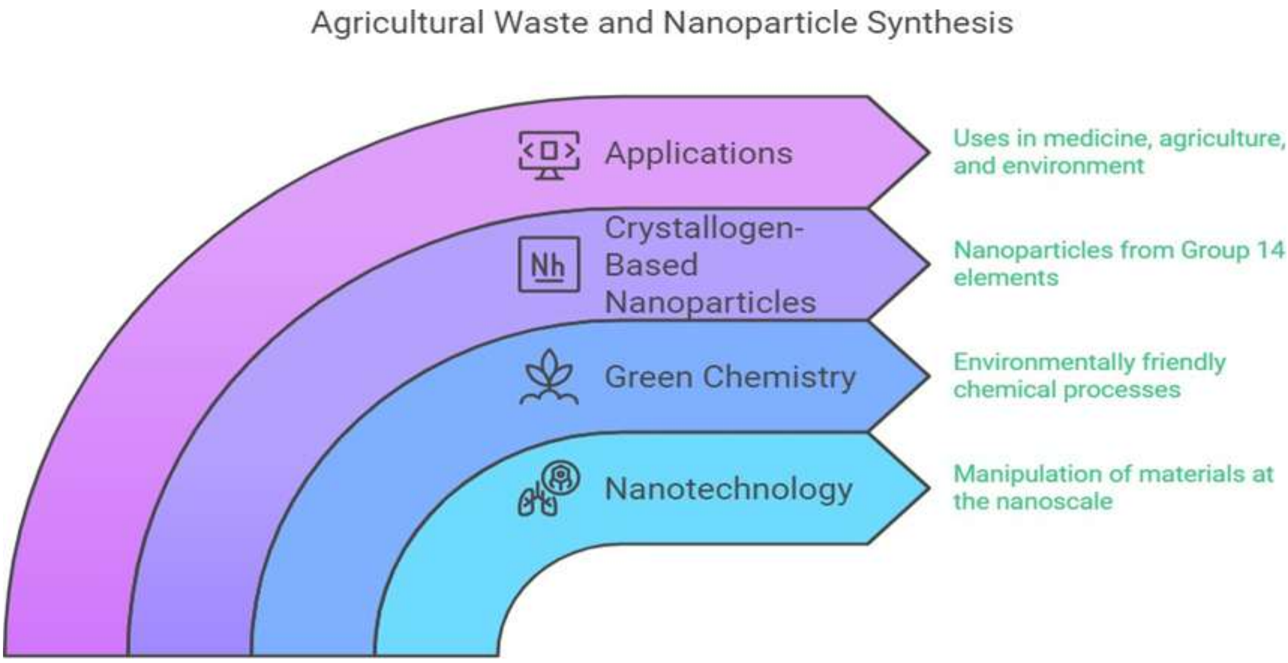

Fig. 1. Scientific representation of agricultural waste and nanotechnology integration.

2. Results and discussion

Methods for Nanoparticles Synthesis

The production, functionalization, and uses of metallic, semiconductor, magnetic, and multifunctional nanoparticles are the main topics of this area. This study is not intended to be a comprehensive compilation of all the literature; rather, we provide common and illustrative examples to facilitate discussions on the synthesis, functionalization, and uses of those nanoparticles. To guarantee the manufacturing of environmentally friendly nanoparticles, each method's sustainability and environmental impact must be carefully considered. The method of choosing is determined by the intended use and desired attributes of the nanoparticles.

Chemical Reduction

Chemical reduction is one of the most preferred methods for synthesizing nanoparticles due to its simplicity, cost-effectiveness, efficiency, and the ability to control structural parameters. This method is widely used because it is easy to perform and is one of the simplest approaches for nanoparticle synthesis (Szczyglewska et al., 2023).

In this method, substrates can be either natural compounds or chemicals, facilitating a reduction reaction. The oxidation or reduction states of the substrates can vary, allowing for diverse applications. The size of the nanoparticles plays a critical role in this process, as controlling the size enables the synthesis of nanoparticles with different morphologies.

The cost-effectiveness of the chemical reduction method makes it suitable for scaling up to large-scale preparation without the need for high pressure, energy, or temperature conditions. This scalability, combined with its simplicity, ensures its continued relevance in nanoparticle synthesis (Goia, 1998; Figure 2).

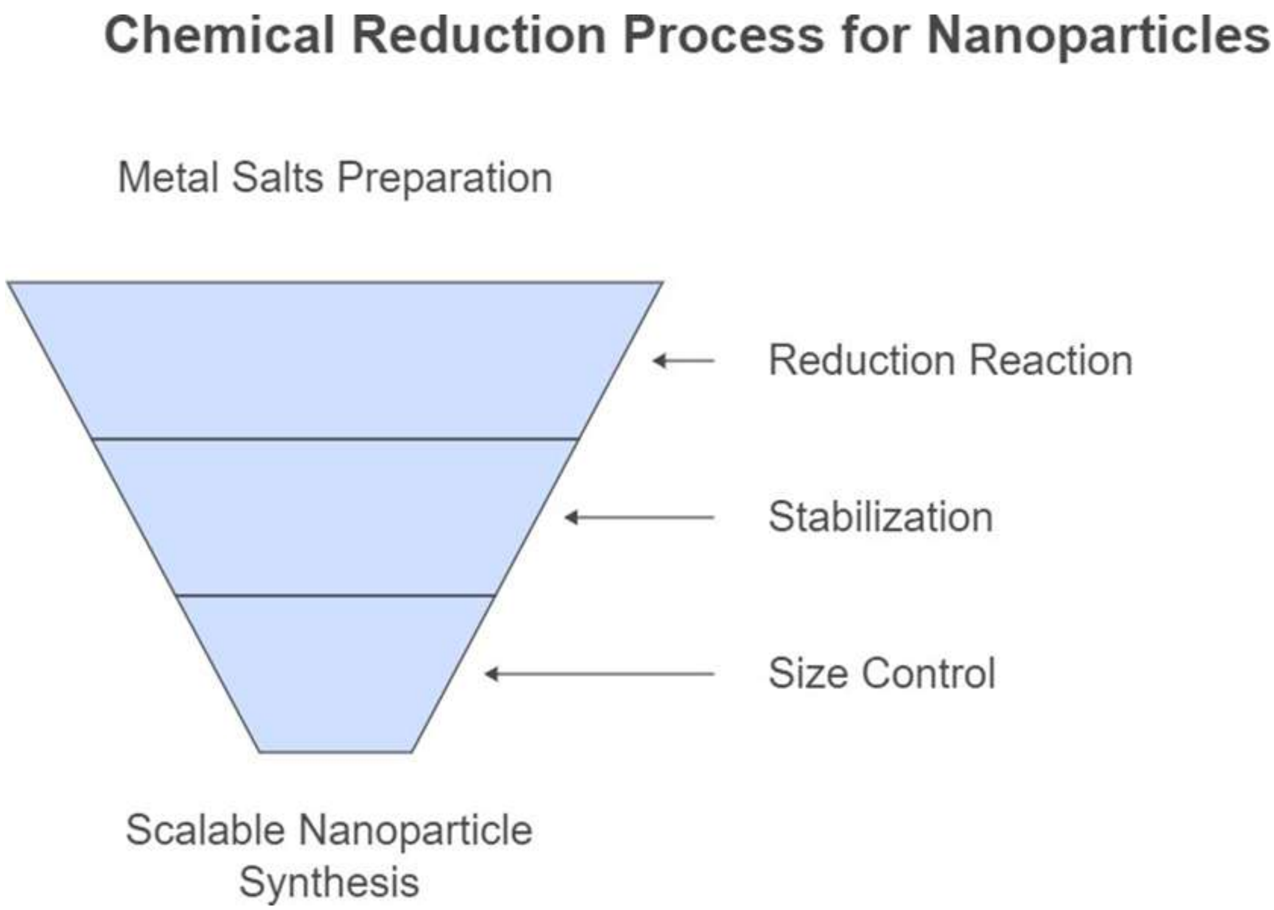

Fig. 2. Schematic representation of the chemical reduction process for synthesizing metal nanoparticles

Using a reducing agent and a stabilizer, salts of a chosen metal are reduced to create metal nanoparticles through chemical reduction (Sharma et al., 2019). The study by Chou and colleagues

(Chou, Ren, 2000) examined the use of silver nitrate in the chemical reduction process to create silver nanoparticles. ($AgNO_3$) as a metal precursor, formaldehyde (CH_2O) as a reducing agent, and polyvinylpyrrolidone/poly (vinyl alcohol), (PVP/PVA) as stabilizing agents. A solution of either sodium carbonate (Na_2CO_3) or sodium hydroxide (NaOH) The ideal pH was ascertained using sodium hydroxide (NaOH). It was investigated how the amount of alkaline solution affected the final nanoparticles shape.

Silver nitrate ($AgNO_3$) and other aqueous salts of metals can be chemically reduced to create zero-valent nanoparticles through a wet-chemical process known as chemical reduction. In order to reduce the precursor metal salt, metal ions must be reduced to zero valence by producing electrons for them by the employment of at least one reducing agent. Reductants including ascorbate, citrate, and borohydride are frequently utilized. A stabilizing agent stabilizes reduced nanoparticles. Cetyltrimethylammonium bromide [($C_{16}H_{33}$)$N(CH_3)_3Br$; CTAB], which is frequently employed in the manufacture of gold nanoparticles, is an illustration of a stabilizing agent. When creating silver nanoparticles, sodium citrate is one example of a reducing agent that can also serve as a stabilizing agent (Aashritha, 2013; Saleh, Alaqad, 2016).

Coprecipitation Method

Several people consider the coprecipitation method to be a standard method for creating magnetic nanoparticles (MNPs) because of its ease of use and efficiency (Guleri et al., 2020; Parmanik et al., 2022; Arsalani et al., 2019). In this chemical process, homogenous solutions containing the ions to be precipitated are combined. Precipitation happens when the target salt's solubility product is surpassed. When a substance's concentration reaches supersaturation during the coprecipitation process, nucleation usually starts suddenly. As more material diffuses onto the surface, nucleation grows and eventually forms nanoparticles. The rate of nucleation in relation to the growth phase needs to be carefully regulated in order to produce homogenous nanoparticles.

Fe_3O_4 nanoparticles are commonly synthesized using this method. A black pre capitate forms when NH4OH is added to a vigorously stirred mixture of $FeCl_2$ and $FeCl_3$ salts, maintaining a Fe^{2+} to Fe^{3+} 1:2 molar ratio at 70°C. After purification, the nanoparticles are collected via magnetic separation and repeatedly washed with ethanol and distilled water to remove residual chemicals (Arsalani et al., 2019; Qu et al., 2013; Dung et al., 2016; Khalil, 2015; Mascolo et al., 2013). Notably, the pH and ion concentration of the solution can influence the size of the resulting nanoparticles.

Despite its widespread use, little is known about the chemical pathways that result in the creation of the magnetite phase in the coprecipitation reaction. Optimizing the control over the crystal structure, morphology, and particle size of magnetite nanoparticles which are widely employed in biological applications requires an understanding of these processes (Ahn et al., 2012).

Microemulsion and Inverse Microemulsion Methods

Another popular method for creating nanoparticles is the use of microemulsion techniques, which take use of the particles' regulated sizes and shapes. An isotropic and thermodynamically stable mixture of water, oil, and surfactants often in combination with cosurfactants is called a microemulsion (Mittal, 2015). These systems serve as soft templates, providing a mildly regulated environment for the creation of nanoparticles.

Microemulsions can be classified into two main types: direct (oil dispersed in water) and reverse (water dispersed in oil). In the reverse microemulsion system, small aqueous-phase droplets (micelles) containing salts or other reactants are stabilized by surfactants in an oil matrix. Nanoparticle formation occurs when these micelles collide and mix, with the surfactant layer controlling the growth of nanoparticles (L´opez-Quintela, Rivas, 1993). For instance, Fe_3O_4 nanoparticles can be synthesized and further functionalized with a silica layer for enhanced stability and biocompatibility. This method is also used to prepare core shell structures, such as Fe_3O_4/Au nanoparticles, which prevent oxidation and enhance functionality (Feltin, Pileni, 1997).

The capacity to produce multifunctional nanoparticles makes the inverse microemulsion technique very noteworthy. Single nanoparticles are encapsulated within silica matrices that are created in the aqueous phase during this process (Dung et al., 2016). Numerous sectors, such as wound healing, oncology, cosmetology, and the creation of antiviral and antibacterial drugs, heavily rely on microemulsions (Nikolaev et al., 2023). These systems' thermodynamic stability permits uniform droplet production, and their stability is determined by molecular interactions within nanodomains.

Hydrothermal Method

Since its first use in geological study in the middle of the 19th century, the hydrothermal process has grown to become a commonly used technique for creating nanoparticles. With this technique, high-temperature and high-pressure conditions are created while reactions are carried out in an aqueous solution inside a closed reaction vessel. Substances that are normally insoluble or slightly soluble dissolve and recrystallize in these conditions (Yang, Park, 2019). Byrappa and Yoshimura (2007) state that the hydrothermal approach uses heterogeneous reactions at high pressures and temperatures to help create nanoparticles from insoluble chemicals. Usually, the procedure takes place in an autoclave, which is a steel pressure vessel that is filled with water and the required reactants. In general, hydrothermal synthesis doesn't require temperatures higher than 300°C. Supersaturation and increased reaction rates under these conditions promote the formation of nanoparticles.

Metal oxide nanoparticles, metal nanoparticles, and semiconductor nanoparticles have all been produced using this method extensively. For instance, the hydrothermal approach is frequently used to create carbon quantum dots (CQDs) with a consistent size distribution and a variety of surface functionalization (such as oxygen, nitrogen, or sulfur groups) (Li et al., 2011; Liu et al., 2018; Wang et al., 2018). Furthermore, metal oxide nanoparticles have been created under supercritical water conditions (Hayashi, Hakuta, 2010), and this method has also been successfully utilized to make metal (Kim et al., 2014) and semiconductor nanoparticles (Van Bui et al., 2014).

The hydrothermal method is a preferred technique in the synthesis of advanced materials because of its versatility and capacity to yield high-quality nanoparticles. This method is very much provided in the described type in the Figure 3 below.

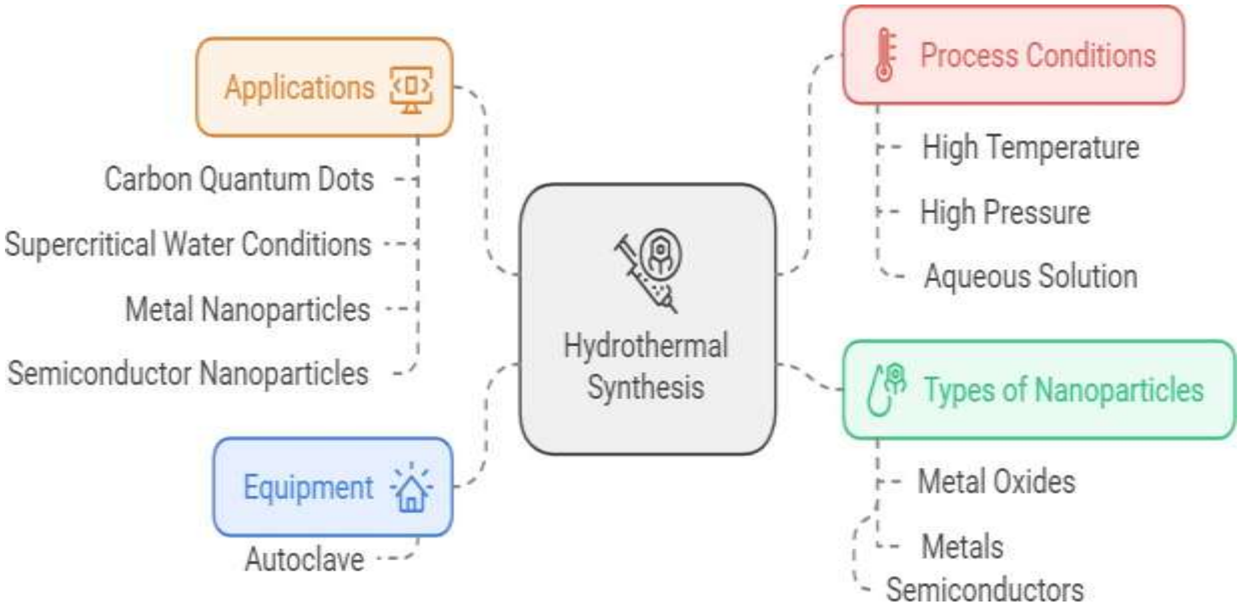

Fig. 3. Overview of Hydrothermal Synthesis: Applications, Process Conditions, Equipment, and Nanoparticle Types

Carbon Based Nanoparticles

Carbon is the very first element of the crystallogens. The usage of carbon in the agricultural industry extends far beyond basic applications. Carbon is essential due to its role in the photosynthetic process where plants use sunlight and air to release oxygen. It serves as nutrition for other animals and as a free energy source for soil microbial processes found in nature. The energy from plants and animals that we consume provides nourishment for soil microbes that supply plants with nutrients. It is present in plant roots, which give soil bacteria sustenance and help prevent soil erosion by giving regenerating soils structure.

Carbon accelerates the process by which nutrients are cycled back to young plants and is a major component of microbial glues that create soil structure, crucial for soil resilience. Additionally, it enhances water infiltration and water retention capacity (South Dakota..., 2024).

Carbon-based nanoparticles have gained significant importance over the last few decades. The discovery of Buckminster (C60) fullerenes in 1985 opened a new class of carbon chains which can be synthesized and produced. This class includes fullerenes, nano-onions, nano-cones, nano-horns, carbon dots, and carbon nanotubes (CNTs) (Mukherjee et al., 2016). Carbon nanoparticles are distinguished from regular carbon materials by their remarkable surface area, mechanical strength, electrical conductivity, low toxicity, biocompatibility, and thermal stability (Thippeswamy et al., 2021).

Many synthetic processes prepare carbon nanomaterials in different sizes, shapes, and chemical compositions. Chemical vapor deposition (CVD), which employs expensive ingredients like ethylene and carbon monoxide, is a common commercial process for producing carbon nanoparticles (CNPs) (Rajput et al., 2015; Zhao et al., 2020). CVD is the most used technique for the production of carbon nanotubes due to its lower temperature requirement, making the process more cost-effective compared to other methods. Additionally, CVD allows for control over the morphology and structure of the produced nanotubes (Manawi et al., 2018) making it a suitable candidate compared to earlier techniques like laser ablation (Guo et al., 1995) and electric arc discharge, both of which involve relatively higher temperatures (Journet et al., 1997).

Despite its effectiveness, CVD is not green and causes significant pollution due to the use of ethylene and carbon monoxide vapors, making the technique expensive. Therefore, carbon nanoparticles are now being synthesized from various agricultural wastes. For example, nitrogen-based carbon nanoparticles have demonstrated metal free electrocatalytic and glucose sensing activity (Li et al., 2015). Similar electrochemical sensors were observed when onion peel extract was used (Akshaya et al., 2019).

As for animal wastes, cow dung has been used to produce eco-friendly, cost-effective conductive paint (CP) (Bhakare et al., 2020). The wide range of applications of carbon-based nanoparticles can be attributed to the ability of carbon nanomaterials to form very strong bonds with objects lighter than them or with themselves. Carbon black or nanospheres derived from waste extract are used as nanofilters in different polymer matrices (Pace, 2001). Recent trends indicate that pyrolysis methods are gaining significant importance in carbon nanoparticle formation (Lee et al., 2017; Wibowo et al., 2015). This method uses a mixture of carbon dioxide along with methane and hydrogen. Agricultural wastes are reduced in size and subjected to high temperatures of about 500°C (Alaya et al., 2000; Jirimali et al., 2022).

Another method used for nanoparticle formation is hydrothermal synthesis, which converts agricultural wastes to fuels and carbon-based nanomaterials (Sharma et al., 2020). For example, collected samples of banana peels are placed in a hydrothermal reactor for 6 hours, where three major steps occur: material dehydration to produce furfural derivatives, followed by polymerization of the modified product, and finally, dehydration. The obtained product is then centrifuged to obtain banana peel carbon (Allwar et al., 2018).

The methods of preparation of various agricultural wastes are summarized in Table 1.

Table 1. Nanocarbon Production Methods from Various Agricultural Wastes

Agricultural Waste	Raw Material Preparation	Method	References
Pineapple Solid Biomass	Rinsed with hot deionized water, dried at 110 °C, cut into small pieces	Activated with zinc chloride, dried at 100°C, carbonized at500 °C	Nizamuddin et al., 2019; Mahamad et al., 2015
Pineapple Crown	Rinsed with deionized water, dried in sunlight, pre-carbonized at 50-250 °C	Activated with potassium hydroxide, pyrolyzed at 30-500 °C under inert atmosphere	Taer, Taslim, 2018; Taer et al., 2019
Rice Husk	Washed with distilled water, dried at 65 °C, ground into fine powder	Activated with ferrocene and ethanol, microwaved at 600 W, carbonized at 800-900 °C	Asnawi et al., 2018; Liou, 2004; Raman et al., 2017

Agricultural Waste	Raw Material Preparation	Method	References
Date Palm	Cleaned with deionized water, dried at 100-110 °C	Activated with an activator, boiled at 600-800 °C under N2 atmosphere	Hussein et al., 2015
Nicotiana Tabacum Stems	Cut into small pieces, dried at 105°C, impregnated with KOH	Carbonized,in muffle furnace under inert atmosphere, rinsed with HCl, dried at 105 °C	Musuna-Garwe et al., 2018
Sugarcane Bagasse	Collected in fiber form, cut into small pieces, impregnated with reagent	Pyrolyzed at 600-1000°C using generated gases	Alves et al., 2012
Orange Peel	Collected, activated with KOH, pyrolyzed	Activated at 600-800°C, K_2CO_3 decomposed, reacted to form hollow channels	Ranaweera et al., 2017

Silicon Nanoparticles from Agricultural Waste

Silicon is the 2nd element of group 14 of periodic table. When given as a fertilizer to certain soils, silicon is advantageous to a wide variety of crops. Although horsetail (Equisetum) and certain forms of algae require silicon from the environment to survive, most plants do not consider it to be an essential ingredient. Many plant species, particularly grasses, are able to absorb silicon at levels similar to those of macronutrients. The plant's high silicon concentration enhances its mechanical strength. In addition to its structural function, silicon can strengthen a plant's defensive mechanism against disease, pests, and environmental stress. Fertilizing soils with silicon boosts crop yields for certain crops, even in the absence of disease and under ideal growth conditions (Rutgers New..., 2018).

Silicon nanoparticles can be synthesied in both highly acidic and basic conditions by using quaternary alkylammonium surfactants, pluronic F127, P123 respectively (Beck et al., 1992; Kresge et al., 1992; Huo et al., 1994). The non-porous silica naroparticles core chemically synthesized by thermal method in which silicais burnt to form SiO_2 molecules. This method is also known as Aersol method (Panas et al., 2014; Mebert et al., 2017). On the other hand, another method called precipitation method is no adopted when an alkali-metal silicate (Rasmussen et al., 2013). Agricultural wastes have a high core of silicon content.

Crop residue like Grrain Cheff, Sugar Molasses and coconut hulls are presently being employed in the silicon nanoparticle synthesis. Water pollution is presently a topic of global concern can be addressed by the production of silicon nanoparticles (Akhayere et al., 2022; Shinde et al., 2021).

Agricultural Waste

Products from agriculture waste are used as fuel, to make green fertilizers, and occasionally to extract useful compounds. The production of SiNPs uses the agricultural waste as a precursor. Utilizing agricultural waste has several benefits, the primary one being its plentiful supply at the conclusion of each harvest season. Therefore, as compared to other approaches, nanoparticle production techniques that make use of agricultural wastes are always more cost-effective.

One agricultural waste product that contains large amounts of silica is rice husk. The usage of this material to create high-quality SiNPs has been the subject of numerous reports in the literature. For example, silica micro- and nanoparticles were first produced using rice hull by Jansomboon et al. (2017), Lu et al. (2024) manufactured very pure amorphous silica nanodiscs using rice straw as a source of silica. SiNPs were made from sugarcane bagasse, a significant waste product from the sugar industry. This environment friendly method provides an affordable means of utilizing agricultural waste. Seoka et al. created SiNPs and nano-silicon via magnesiothermic processes and SUGARCANE bagasse ash (Seroka et al., 2022). Using sticky, red, and brown rice husk ash, Sankar et al. created biogenerated SiNPs using a basic scheme of silica nanoparticles (Sankar et al., 2016).

Other Agricultural Waste Sources

In order to extract 52-78 % silica from various agricultural wastes, such as rice husk, bamboo leaves, sugarcane bagasse, and groundnut shellused to synthesized SiNPs (Akhayere et al., 2022). Through the use of annelid bioprocessing, crystalline SiNPs from agricultural waste produced. After generating humus from these agro-wastes employing *Eisenia foetida* species, SiNPs were obtained by calcination and acid treatment (Esp´ındola-Gonzalez et al., 2010). Using sedge (*Carex riparia*), which generates a lot of agro-waste, an innovative way to synthesize silica nanoparticles were reported (Costa, Paranhos, 2020). Naidu et al. (Naidu et al., 2023) synthesized silica nanoparticles for the food industry using sorghum residues, which contain significant levels of silica.

Table 2. Silicon Nanoparticles Synthesized using Other Agricultural Waste Sources

Source	Method	Reference
Rice husk, bamboo leaves, sugarcane bagasse, groundnut shell	-	Akhayere et al., 2022
Eisenia foetida treated agrowastes	Calcination, acid treatment	Esp´ındola-Gonzalez et al., 2010
Carex riparia	-	Costa, Paranhos, 2020
Sorghum residues	-	Naidu et al., 2023

Tin Oxide Nanoparticles from Plant-Mediated Synthesis

Plant-mediated synthesis has become a sustainable and cost-effective alternative for synthesizing nanoparticles, offering significant advantages over traditional physico-chemical methods. These green approaches eliminate the need for toxic chemicals, high temperatures, and high-pressure conditions, providing naturally sourced reducing and stabilizing agents. Moreover, the plant extracts allow the large-scale production of stable, uniform nanoparticles.

Several studies have explored various plant species for the green synthesis of tin oxide (SnO_2) nanoparticles, producing NPs with different morphologies and sizes depending on the specific plant extract and reaction conditions. The general process involves dissolving a tin salt in the plant extract, followed by centrifugation, drying, and thermal treatment to obtain the final product. Several plant-mediated syntheses of SnO_2 NPs have been reported, highlighting their application in photocatalysis and antibacterial activity. Table 3 summarizes notable studies in the literature.

The green synthesis of SnO_2 NPs has been shown to result in varying nanoparticle sizes and morphologies, depending on the specific plant species and conditions used. For instance, *Aspalathus linearis* yielded quasi-spherical particles with sizes ranging from 2.5 to 11.4 nm, while *Aloe barbadensis miller* produced larger particles ranging from 50 to 100 nm (Diallo et al., 2016; Selvakumari et al., 2017; Haritha et al., 2016; Gowri et al., 2013).

Table 3. Plant-Mediated SnO_2 Nanoparticles Synthesis

Plant Species	Precursor	Size, nm	Application
Aspalathus linearis (Diallo et al., 2016)	$SnCl_4·5H_2O$	2.5–11.4	Antibacterial Photocatalytic
Camellia sinensis Selvakumari et al., 2017)	$SnCl_4·5H_2O$	5–30	Photocatalytic
Catunaregam spinosa (Haritha et al., 2016)	$SnCl_2·2H_2O$	47	Dye Degradation
Aloe barbadensis miller (Gowri et al., 2013)	$SnCl_2·2H_2O$	50–100	Antibacterial
Plectranthus amboinicus (Fu et al., 2015)	$SnCl_2·2H_2O$	63	Photocatalytic
Nyctanthes arbortristis (Rajiv Gandhi et al., 2012)	$SnCl_2·2H_2O$	2–8	Hydrolysis Capping

Plant Species	Precursor	Size, nm	Application
Psidium guajava (Kumar et al., 2018)	$SnCl_4 \cdot 5H_2O$	8–10	Dye Degradation
Calotropis gigantea (Bhosale et al., 2018)	$SnCl_4 \cdot 5H_2O$	30–40	Dye Degradation
Piper betle (Singh et al., 2018)	$SnCl_4 \cdot 5H_2O$	8.4	Selective Dye Degradation

Lead Nanoparticles in Agriculture

Lead, the heaviest element in Group 14, plays a critical role in agriculture due to its detrimental effects, such as inhibiting photosynthesis, disrupting water balance, and altering membrane permeability in plants. The uptake of lead by plants is influenced by factors including particle size, root exudation, and various physical and chemical processes (Nas, Ali, 2018). Lead exists in various forms, including lead monoxide (PbO), lead dioxide (PbO_2), and lead(III) oxide (Pb_2O_3), with PbO being the most extensively studied due to its widespread use in industries such as batteries, gas production, and as a catalyst in organic chemistry (Panas et al., 2014; Rangaraj, Venkatachalam, 2017; Alshatwi et al., 2015).

Lead nanoparticle synthesis can be achieved via three main approaches: chemical, physical, and green (biological) methods. Techniques such as chemical synthesis, calcination, sol-gel pyrolysis, thermal breakdown, chemical deposition, and microwave irradiation have recently been developed to produce PbO nanostructures (Bratovcic, 2020). Bio-synthesis is particularly promising as it may enhance the properties of PbO nanoparticles while reducing the production of toxic by-products during synthesis (Rokade et al., 2016; Sharar, Bozeya, 2017). This method could offer an environmentally friendly alternative to traditional approaches for creating metal oxide nanoparticles.

Despite the significant potential of lead oxide nanoparticles, the environmental impact of PbO pollution remains a major concern. Lead oxide's substantial negative influence on ecosystems necessitates the development of effective solutions for managing lead pollution. Nanotechnology and biosynthesis may offer solutions by creating safer forms of lead nanoparticles. Recent research demonstrates that biosynthesis, including the use of natural gelatin-based stabilizers, can effectively produce PbO NPs, as discussed in recent work (Narayanan, 2012; Miri et al., 2018). However, the synthesis of PbO NPs from agro-waste remains an open area for further exploration.

Characterisation of NMs from Agro-Wastes

Value-added product production with minimal impact on the environment can be achieved by the production of nanomaterials (NMs) from agricultural waste. The abundance and renewable nature of agro-waste, which includes agricultural leftovers like fruit peels, rice husks, and sugarcane bagasse, make it a suitable feedstock for the synthesis of nanomaterials. To comprehend these NMs' physicochemical characteristics and possible uses, characterization is essential. With an emphasis on the structural, morphological, and functional characteristics of the nanomaterials made from agricultural waste, this section addresses the methods and procedures utilized to analyse them.

Fourier Transform Infrared Spectroscopy (FTIR)

By measuring the amount of absorbed energy and comparing it to a database, FTIR can be used to identify the functional groups that are present and characterize the chemical structure of the sample. FTIR spectroscopy is a very efficient and non-destructive method for analyzing the chemical and physical properties of lignocellulosic biomass (Guerrero-P´erez, Patience, 2020). Plant fiber is primarily composed of three components: cellulose, lignin, and hemicellulose. The literature has made considerable use of FTIR to verify the removal of amorphous sections such as hemicellulose and lignin from the fiber matrix following chemical treatments such as bleaching and alkali treatment, or to determine whether any lignin or hemicellulose is present in the extracted cellulose nanofibres. Chirayil et al. (2014) examined fibres that had been bleached, acid-treated, alkaline-treated, and left untreated using FTIR spectroscopy. They discovered a peak in each fiber's spectra at 3300 cm^{-1}. The hydrophilic character of the fibers was shown by this peak, which matched the OH stretching vibrations of the hydrogen-bonded hydroxyl group.

According to Lima et al. (2023), FTIR analyses of the CNs produced from banana peel through enzymatic treatment yielded similar results. They were able to show that hemicellulose and lignin were successfully extracted from the fiber matrix by the enzymatic treatment. Bleaching was apparently used to remove the majority of the lignin in the banana peel cellulose nanofibres, according to Zope et al. (2022). Isolation The vibrations at 1238 per cm (guaiaryl ring respiration with stretching C=O), 1525 per cm (aromatic ring vibrations), and 761 per cm (C-H deformations) disappeared after bleaching. Karimi et al. (2014) examined the FTIR of samples of unbleached (UBNF) and bleached (BNF) kenaf bast cellulosic fiber and discovered that lignin was absent from both UBNF and BNF samples.

X-ray Photoelectron Spectroscopy (XPS)

XPS is a surface analysis technique that offers comprehensive insights into the chemical composition and states of a wide range of materials. Few XPS research have been conducted on cellulose nanofibres. Ahola et al. (2008) examined model films constructed of cellulose nano-fibrils using XPS in one study. They discovered that the surface was coated with cellulose nano-fibrils after spin-coating cellulose nano-fibril dispersions onto silica substrates to form these films.

In another work, the chemical composition of nano-fibrillated cellulose aerogels and films was examined by Zuo et al. (2019) both before and after coating them with a substance known as perfluorodecyl trichlorosilane (PFOTS). They discovered that carbon, oxygen, and trace levels of salt were present on the first cellulose surface. Following PFOTS coating, silicon, fluorine, were also present, indicating that PFOTS had interacted with the cellulose.

Measurements of the Zeta-Potential of Agriculture-Based NPs

The stability of suspensions containing cellulose nanofibers depends on the zeta potential. It gauges how much a liquid's particles oppose one another, keeping them uniformly distributed.

Dominic and colleagues' study (Dominic et al., 2022). They took measurements of the zeta potential of suspensions of banana peel-derived cellulose nanofibre (CN). With zeta potential values ranging from 16.2 to 44.2 mV, they produced extremely stable CN suspensions by subjecting the CNs to a high-pressure homogenizer many times. Surattanamal et al. (2022) found that the zeta potential of the nanofibers obtained by enzymatic and chemical treatment were respectively. They found that cellulose nanofibres with the greatest zeta capacity and higher electrical conductivity were generated via enzymatic therapy as opposed to chemical treatment.

Li and colleagues' study (2013), by measuring the water contact angles, they examined the hydrophilicity (the ability to repel water) of various starches. Additionally, they evaluated the zeta potential of starch granules and discovered that the values for rice, waxy maize, wheat, and potato starch were −20.5, −19.1, −20.4, and −4.2 mV, respectively. Wei and colleagues' study (2014), they noticed that the zeta potential dropped from −6.7 to −34.5 mV as the pH of the starch dispersion rose from 2.07 to 11.96. Furthermore, as the pH rose, the starch nanocrystal distribution widened.

Other Applications

Nano-Biosensors

NPs, plant fractions, soil, water, and nanotubes, nanowires, or nanocrystals in the agro-ecosystem are all monitored by NBSs. Using the physic-chemical properties of NMs, NBSs offer a potent tool compared to existing analytical sensors and biosensors that combine biological element detection with chemical or physical principles. Biological data is converted by a transducer into a signal that can be generated by an electrical device. With this skill, an agronomist may precisely and promptly keep an eye on the dietary and water requirements of the crops as well as any early indicators of illness (Mendes et al., 2020). For plant science research, high-resolution crop monitoring with nano-biosensors may be a highly helpful instrument.

Use of Nano-Fertilisers

Recent agricultural research has increasingly focused on micronutrients while some – what neglecting the critical role of macronutrients like nitrogen (N), phosphorus (P), and potassium (K) in influencing crop productivity. However, it's widely recognized that these macronutrients play a foundational role in supporting robust plant growth and yield. International and national organizations advocating for sustain- able agricultural practices and food security emphasize the importance of reorienting nanotechnology applications in agriculture towards developing nano-fertilizers specifically tailored to enhance the availability and efficiency of N and P. This shift aims to address pressing global challenges related to agricultural sustainability by ensuring that essential macronutrients are effectively utilized to meet growing food demands.

Nano-Fungicides

Fungi are mostly responsible for agricultural damage, including that to significant crops like rice, wheat, barley, groundnuts, and cotton (Neme, Mohammed, 2017). Fungicides can harm biodiversity, prompting the need for alternative strategies against fungal diseases. NPs, such as silver (Ag-NPs), copper (Cu-NPs), zinc oxide (ZnO-NPs), and magnesium oxide (MgO-NPs), have shown promising antifungal properties. Ag-NPs effectively reduce infections from fungi like *Magnaporthe grisea* and *Bipolaris sorokiniana*, while Cu-NPs and Ag-NPs inhibit *Alternaria alternata* and *Botrytis cinerea*. ZnO-NPs and MgO-NPs combat Rhizopus stolonifer, *Fusarium oxysporum*, and *Mucor plumbeus* (Bhattacharjee et al., 2022). Additionally, pesticides like zineb and mancozeb, when encapsulated in a MWCNT-g-PCA hybrid, demonstrate enhanced efficacy, with mancozeb particularly effective against *Alternaria alternata* (Nath et al., 2023).

3. Conclusion and Future Directions

The field of nanotechnology has demonstrated significant potential across various sectors, including agriculture, through the application of nanoparticles such as those based on carbon, silicon, and lead. Carbon-based nanoparticles, with their unique properties like high surface area, mechanical strength, and electrical conductivity, have enhanced soil structure, water retention, and nutrient cycling. Economical and environmentally friendly methods, such as chemical vapor deposition, pyrolysis, and hydrothermal synthesis, have been instrumental in their production, particularly from agricultural wastes. Silicon nanoparticles (SiNPs) derived from agricultural residues offer a sustainable and cost-effective solution for green fertilizers and plant growth enhancement. This approach not only addresses waste management challenges but also promotes sustainable agricultural practices. Similarly, while lead nanoparticles have been extensively studied for their industrial applications, their toxicological effects require further research to develop safe and effective uses in agriculture.

Looking ahead, the field of nanoparticle synthesis using biological organisms holds significant promise for future advancements. Research should explore novel microbial species from diverse and extreme environments, which may enable the synthesis of nanoparticles with unique properties. Genetic engineering and synthetic biology approaches can enhance the efficiency and specificity of nanoparticle synthesis, paving the way for engineered strains and custom-designed biosynthetic pathways. Mechanistic studies aimed at elucidating the molecular and biochemical processes involved in microbial nanoparticle synthesis will be vital for optimizing production methods and unlocking new biotechnological applications. Scaling up laboratory-scale synthesis to industrial production presents a critical challenge. Future research must focus on developing scalable, cost-effective processes for large-scale nanoparticle synthesis and integrating these processes into existing industrial frameworks. Furthermore, comprehensive studies on the environmental and health impacts of biologically synthesized nanoparticles are essential to ensure their safe and sustainable application. Long-term assessments of stability, biocompatibility, and toxicity will be crucial for mitigating risks and maximizing the benefits of nanotechnology. In conclusion, the integration of nanotechnology in agriculture and other industries offers immense opportunities for innovation and sustainability. Continued research and development, particularly in the areas of green synthesis and application of nanoparticles, will be essential to fully realize their potential while addressing associated challenges and ensuring safety for ecosystems and human health.

4. Declarations

Funding: There is no funding for this project.
Competing interests: There is no conflict of interest.
Data availability: Not applicable.

5. Author contribution

The study on silicon nanoparticles was done by Prachi Kurhade along with the section of characterisation was developed by her. Himanshu formulated the study on carbon nanoparticles and the application and Priyadrahsni Rajput and Sakshi Singh contributed in writing, editing and finalizing this work.

6. Acknowledgements

Priyadarshani Rajput acknowledges the support by the Strategic Academic Leadership Program of the Southern Federal University ("Priority 2030"). Himanshu Bansal acknowledges the support from Ms. Prajakta Ghatge over her inputs in the biological process section editing.

References

Aashritha, 2013 – *Aashritha, S.* (2013). Synthesis of silver nanoparticles by chemical reduction method and their antifungal activity. *International Research Journal of Pharmacy*. 4(10).

Ahn et al., 2012 – *Ahn, T., Kim, J.H., Yang, H.-M., Lee, J.W., Kim, J.-D.* (2012). Formation pathways of magnetite nanoparticles by coprecipitation method. *The Journal of Physical Chemistry C*. 116(10): 6069-6076.

Ahola et al., 2008 – *Ahola, S., Salmi, J., Johansson, L.-S., Laine, J., Osterberg, M.* (2008). Model films from native cellulose nanofibrils. preparation, swelling, and surface interactions. *Biomacromolecules*. 9(4): 1273-1282.

Akhayere et al., 2022 – *Akhayere, E., Kavaz, D., Vaseashta, A.* (2022). Efficacy studies of silica nanoparticles synthesized using agricultural waste for mitigating waterborne contaminants. *Applied Sciences*. 12(18). DOI: https://doi.org/10.3390/app12189279.

Akhayere et al., 2022 – *Akhayere, E., Kavaz, D., Vaseashta, A.* (2022). Efficacy studies of silica nanoparticles synthesized using agricultural waste for mitigating waterborne contaminants. *Applied Sciences*. 12(18): 9279.

Akshaya et al., 2019 – *Akshaya, K., Bhat, V.S., Varghese, A., George, L., Hegde, G.* (2019). Non-enzymatic electrochemical determination of progesterone using carbon nanospheres from onion peels coated on carbon fiber paper. *Journal of the Electrochemical Society*. 166(13): 1097.

Alaya et al., 2000 – *Alaya, M., Girgis, B., Mourad, W.* (2000). Activated carbon from some agricultural wastes under action of one-step steam pyrolysis. *Journal of Porous Materials*. 7: 509-517.

Allwar et al., 2018 – *Allwar, A., Febriyantri, H.Z., Yuliantari, R.* (2018). Research article preparation and characterization of hydrothermal activated carbon from banana empty fruit bunch with ZnCl2 activation for removal of phenol in aqueous solution.

Alshatwi et al., 2015 – *Alshatwi, A.A., Athinarayanan, J., Periasamy, V.S.* (2015). Biocompatibility assessment of rice husk-derived biogenic silica nanoparticles for biomedical applications. *Materials Science and Engineering: C*. 47: 8-16.

Alves et al., 2012 – *Alves, J.O., Ten´orio, J.A.S., Zhuo, C., Levendis, Y.A.* (2012). Characterization of nanomaterials produced from sugarcane bagasse. *Journal of Materials Research and Technology*. 1(1): 31-34.

Arsalani et al., 2019 – *Arsalani, S., Guidelli, E.J., Silveira, M.A., Salmon, C.E., Araujo, J.F., Bruno, A.C., Baffa, O.* (2019). Magnetic Fe_3O_4 nanoparticles coated by natural rubber latex as MRI contrast agent. *Journal of Magnetism and Magnetic Materials*. 475: 458-464.

Asnawi et al., 2018 – *Asnawi, M., Azhari, S., Hamidon, M.N., Ismail, I., Helina, I.* (2018). Synthesis of carbon nanomaterials from rice husk via microwave oven. *Journal of Nanomaterials*. 2018(1): 2898326.

Beck et al., 1992 – *Beck, J.S., Vartuli, J.C., Roth, W.J., Leonowicz, M.E., Kresge, C.T., Schmitt, K.D., Chu, C.T., Olson, D.H., Sheppard, E.W., McCullen, S.B., et al.* (1992). A new family of mesoporous molecular sieves prepared with liquid crystal templates. *Journal of the American Chemical Society*. 114(27): 10834-10843.

Bhakare et al., 2020 – *Bhakare, M.A., Wadekar, P.H., Khose, R.V., Bondarde, M.P., Some, S.* (2020). Eco- friendly biowaste-derived graphitic carbon as black pigment for conductive paint. *Progress in Organic Coatings*. 147: 105872.

Bhattacharjee et al., 2022 – *Bhattacharjee, R., Kumar, L., Mukerjee, N., Anand, U., Dhasmana, A., Preetam, S., Bhaumik, S., Sihi, S., Pal, S., Khare, T. et al.* (2022). The emergence of metal oxide nanoparticles (NPs) as a phytomedicine: A two-facet role in plant growth, nano-toxicity and anti-phyto-microbial activity. *Biomedicine & Pharmacotherapy*. 155: 113658.

Bhosale et al., 2018 – *Bhosale, T., Shinde, H., Gavade, N., Babar, S., Gawade, V., Sabale, S., Kamble, R., Shirke, B., Garadkar, K.* (2018). Biosynthesis of SnO2 nanoparticles by aqueous leaf extract of *Calotropis gigantea* for photocatalytic applications. *Journal of Materials Science: Materials in Electronics*. 29: 6826-6834.

Bratovcic, 2020 – *Bratovcic, A.* (2020). Synthesis, characterization, applications, and toxicity of lead oxide nanoparticles. *Lead Chemistry*. 10.

Byrappa, Adschiri, 2007 – *Byrappa, K., Adschiri, T.* (2007). Hydrothermal technology for nanotechnology. *Progress in Crystal Growth and Characterization of Materials*. 53(2): 117-166.

Chirayil et al., 2014 – *Chirayil, C.J., Joy, J., Mathew, L., Mozetic, M., Koetz, J., Thomas, S.* (2014). Isolation and characterization of cellulose nanofibrils from *Helicteres isora* plant. *Industrial Crops and Products*. 59: 27-34.

Chou, Ren, 2000 – *Chou, K.S., Ren, C.Y.* (2000). Synthesis of nanosized silver particles by chemical reduction method. *Materials Chemistry and Physics*. 64(3): 241-246.

Costa, Paranhos, 2020 – *Costa, J.A.S., Paranhos, C.M.* (2020). Mitigation of silica-rich wastes: an alternative to the synthesis eco-friendly silica-based mesoporous materials. *Microporous and Mesoporous Materials*. 309: 110570.

Diallo et al., 2016 – *Diallo, A., Manikandan, E., Rajendran, V., Maaza, M.* (2016). Physical & enhanced photocatalytic properties of green synthesized SnO2 nanoparticles via *Aspalathus linearis*. *Journal of Alloys and Compounds*. 681: 561-570.

Dominic et al., 2022 – *Dominic, C.M., Raj, V., Neenu, K., Begum, P.S., Formela, K., Saeb, M.R., Prabhu, D.D., Vijayan, P.P., Ajithkumar, T., Parameswaranpillai, J.* (2022). Chlorine- free extraction and structural characterization of cellulose nanofibers from waste husk of millet (*Pennisetum glaucum*). *International Journal of Biological Macromolecules*. 206: 92-104.

Dung et al., 2016 – *Dung, C.T., Quynh, L.M., Linh, N.P., Nam, N.H., Luong, N.H.* (2016). Synthesis of ZnS: Mn–Fe_3O_4 bifunctional nanoparticles by inverse microemulsion method. Journal of Science. *Advanced Materials and Devices*. 1(2): 200-203.

Esp´ındola-Gonzalez et al., 2010 – *Esp´ındola-Gonzalez, A., Mart´ınez-Hern´andez, A., Angeles-Ch´avez, C., Castano, V., Velasco-Santos, C.* (2010). Novel crystalline SiO2 nanoparticles via annelids bio- processing of agro-industrial wastes. *Nanoscale Research Letters*. 5: 1408-1417.

Feltin, Pileni, 1997 – *Feltin, N., Pileni, M.* (1997). New technique for synthesizing iron ferrite magnetic nanosized particles. *Langmuir*. 13(15): 3927-3933.

Fritsch et al., 2017 – *Fritsch, C., Staebler, A., Happel, A., Cubero M´arquez, M.A., Aguil´o-Aguayo, I., Abadias, M., Gallur, M., Cigognini, I.M., Montanari, A., L´opez, M.J., et al.* (2017). Processing, valorization and application of bio-waste derived compounds from potato, tomato, olive and cereals: A review. *Sustainability*. 9(8): 1492.

Fu et al., 2015 – *Fu, L., Zheng, Y., Ren, Q., Wang, A., Deng, B.* (2015). Green biosynthesis of SnO2 nanoparticles by *Plectranthus amboinicus* leaf extract their photocatalytic activity toward rhodamine b degradation. *Journal of Ovonic Research*. 11(1): 21-26.

Goia, 1998 – *Goia, D.V., Matijevi´c, E.* (1998). Preparation of monodispersed metal particles. *New Journal of Chemistry*. 22(11): 1203-1215.

Gowri et al., 2013 – *Gowri, S., Gandhi, R.R., Sundrarajan, M.* (2013). Green synthesis of tin oxide nanoparticles by aloe vera: structural, optical and antibacterial properties. *Journal of Nanoelectronics and Optoelectronics*. 8(3): 240-249.

Guerrero-P´erez, Patience, 2020 – *Guerrero-P´erez, M.O., Patience, G.S.* (2020). Experimental methods in chemical engineering: Fourier transform infrared spectroscopy—FTIR. *The Canadian Journal of Chemical Engineering*. 98(1): 25-33.

Guleri et al., 2020 – *Guleri S., Singh, K., Kaushik, R., Dhankar, R., Tiwari, A.* (2020). Phycoremediation: a novel and synergistic approach in wastewater remediation. *Journal of Microbiology, Biotechnology and Food Sciences*. 10(1): 98-106.

Guo et al., 1995 – *Guo, T., Nikolaev, P., Thess, A., Colbert, D.T., Smalley, R.E.* (1995). Catalytic growth of single-walled nanotubes by laser vaporization. *Chemical Physics Letters*. 243(1-2): 49-54.

Haritha et al., 2016 – *Haritha, E., Roopan, S.M., Madhavi, G., Elango, G., Al-Dhabi, N.A., Arasu, M.V.* (2016). Green chemical approach towards the synthesis of SnO2 NPs in argument with photocatalytic degradation of diazo dye and its kinetic studies. *Journal of Photochemistry and Photobiology B: Biology*. 162: 441-447.

Hayashi, Hakuta, 2010 – *Hayashi, H., Hakuta, Y.* (2010). Hydrothermal synthesis of metal oxide nanoparticles in supercritical water. *Materials*. 3(7): 3794-3817.

Huo et al., 1994 – *Huo, Q., Margolese, D.I., Ciesla, U., Feng, P., Gier, T.E., Sieger, P., Leon, R., Petroff, P.M., Schuth, F., Stucky, G.D.* (1994). Generalized synthesis of periodic surfactant/inorganic composite materials. *Nature*. 368(6469): 317-321.

Hussein et al., 2015 – *Hussein, F.H., Halbus, A.F., Lafta, A.J., Athab, Z.H.* (2015). Preparation and characterization of activated carbon from Iraqi Khestawy date palm. *Journal of Chemistry*. 2015(1): 295748.

Jansomboon et al., 2017 – *Jansomboon, W., Boonmaloet, K., Sukaros, S., Prapainainar, P.* (2017). Rice hull micro and nanosilica: synthesis and characterization. *Key Engineering Materials*. 718: 77-80.

Jirimali et al., 2022 – *Jirimali, H., Singh, J., Boddula, R., Lee, J.K., Singh, V.* (2022). Nano-structured carbon: its synthesis from renewable agricultural sources and important applications. *Materials*. 15(11): 3969.

Journet et al., 1997 – *Journet, C., Maser, W.K., Bernier, P., Loiseau, A., La Chapelle, M.L., Lefrant, d.S., Deniard, P., Lee, R., Fischer, J.E.* (1997). Large-scale production of single-walled carbon nanotubes by the electric-arc technique. *Nature*. 388(6644): 756-758.

Karimi et al., 2014 – *Karimi, S., Tahir, P.M., Karimi, A., Dufresne, A., Abdulkhani, A.* (2014). Kenaf bast cellulosic fibers hierarchy: a comprehensive approach from micro to nano. *Carbohydrate Polymers*. 101: 878885.

Khalil, 2015 – *Khalil, M.I.* (2015). Co-precipitation in aqueous solution synthesis of magnetite nanoparticles using iron (iii) salts as precursors. *Arabian Journal of Chemistry*. 8(2): 279-284.

Kim et al., 2014 – *Kim, M., Son, W.-S., Ahn, K.H., Kim, D.S., Lee, H.-s., Lee, Y.-W.* (2014). Hydrothermal synthesis of metal nanoparticles using glycerol as a reducing agent. *The Journal of Supercritical Fluids*. 90: 53-59.

Kresge et al., 1992 – *Kresge, A.C., Leonowicz, M.E., Roth, W.J., Vartuli, J., Beck, J.* (1992). Ordered meso-porous molecular sieves synthesized by a liquid-crystal template mechanism. *Nature*. 359(6397): 710-712.

Kumar et al., 2018 – *Kumar, M., Mehta, A., Mishra, A., Singh, J., Rawat, M., Basu, S.* (2018). Biosynthesis of tin oxide nanoparticles using *Psidium guajava* leave extract for photocatalytic dye degradation under sunlight. *Materials Letters*. 215: 121-124.

L´opez-Quintela, Rivas, 1993 – *L´opez-Quintela, M.A., Rivas, J.* (1993). Chemical reactions in microemulsions: a powerful method to obtain ultrafine particles. *Journal of Colloid and Interface Science*. 158(2): 446-451.

Lee et al., 2017 – *Lee, J., Yang, X., Cho, S.-H., Kim, J.-K., Lee, S.S., Tsang, D.C., Ok, Y.S., Kwon, E.E.* (2017). Pyrolysis process of agricultural waste using CO2 for waste management, energy recovery, and biochar fabrication. *Applied Energy*. 185: 214-222.

Li et al., 2011 – *Li, H., He, X., Liu, Y., Huang, H., Lian, S., Lee, S.-T., Kang, Z.* (2011). One-step ultrasonic synthesis of water-soluble carbon nanoparticles with excellent photoluminescent properties. *Carbon*. 49(2): 605-609.

Li et al., 2013 – *Li, C., Li, Y., Sun, P., Yang, C.* (2013). Pickering emulsions stabilized by native starch granules. *Colloids and Surfaces A: Physicochemical and Engineering Aspects*. 431: 142-149.

Li et al., 2015 – *Li, T., Li, Y., Wang, C., Gao, Z.D., Song, Y.Y.* (2015). Nitrogen-doped carbon nanospheres derived from cocoon silk as metal-free electrocatalyst for glucose sensing. *Talanta*. 144: 1245-1251.

Lima et al., 2023 – *Lima, A.R., Cristofoli, N.L., Costa, A.M.R., Saraiva, J.A., Vieira, M.C.* (2023). Comparative study of the production of cellulose nanofibers from agro-industrial waste streams of *Salicornia ramosissima* by acid and enzymatic treatment. *Food and Bioproducts Processing*. 137: 214-225.

Liou, 2004 – *Liou, T.-H.* (2004). Preparation and characterization of nano-structured silica from rice husk. *Materials Science and Engineering: A*. 364(1-2): 313-323.

Liu et al., 2018 – *Liu, J., Li, D., Zhang, K., Yang, M., Sun, H., Yang, B.* (2018). One-step hydrothermal synthesis of nitrogen-doped conjugated carbonized polymer dots with 31% efficient red emission for in vivo imaging. *Small*. 14(15): 1703919.

Lu et al., 2007 – *Lu, A.H., Salabas, E.E., Schu¨th, F.* (2007). Magnetic nanoparticles: synthesis, protection, functionalization, and application. *Angewandte Chemie International Edition*. 46(8): 1222-1244.

Lu et al., 2024 – *Lu, Y., Jiang, M., Pan, Y., Wang, F., Xu, W., Zhou, Y., Du, X.* (2024). Preparation of Ag@lignin nanotubes for the development of antimicrobial biodegradable films from corn straw. *International Journal of Biological Macromolecules*. 254: 127630.

Madhumitha, 2013 – *Madhumitha, G., Roopan, S.M.* (2013). Devastated crops: multifunctional efficacy for the production of nanoparticles. *Journal of Nanomaterials*. 1: 951858.

Mahamad et al., 2015 – *Mahamad, M.N., Zaini, M.A.A., Zakaria, Z.A.* (2015). Preparation and characterization of activated carbon from pineapple waste biomass for dye removal. *International Biodeterioration & Biodegradation*. 102: 274-280.

Manawi, et al., 2018 – *Manawi, Y.M., Ihsanullah, Samara, A., Al-Ansari, T., Atieh, M.A.* (2018). A review of carbon nanomaterials' synthesis via the chemical vapor deposition (CVD) method. *Materials*. 11(5): 822.

Mascolo et al., 2013 – *Mascolo, M.C., Pei, Y., Ring, T.A.* (2013). Room temperature co-precipitation synthesis of magnetite nanoparticles in a large pH window with different bases. *Materials*. 6(12): 5549-5567.

Mebert et al., 2017 – *Mebert, A.M., Baglole, C.J., Desimone, M.F., Maysinger, D.* (2017). Nanoengineered silica: Properties, applications and toxicity. *Food and Chemical Toxicology*. 109: 753-770.

Mendes et al., 2020 – *Mendes, J., Pinho, T.M., Santos, F., Sousa, J.J., Peres, E., Boaventura-Cunha, J., Cunha, M., Morais, R.* (2020). Smartphone applications targeting precision agriculture practices – a systematic review. *Agronomy*. 10(6): 855.

Miri et al., 2018 – *Miri, A., Sarani, M., Hashemzadeh, A., Mardani, Z., Darroudi, M.* (2018). Biosynthesis and cytotoxic activity of lead oxide nanoparticles. *Green Chemistry Letters and Reviews*. 11(4): 567-572.

Mittal, 2015 – *Mittal, V.* (2015). Synthesis Techniques for Polymer Nanocomposites. John Wiley & Sons.

Mohite et al., 2022 – *Mohite, A.S., Jagtap, A.R., Avhad, M.S., More, A.P.* (2022). Recycling of major agri- culture crop residues and its application in polymer industry: A review in the context of waste to energy nexus. *Energy Nexus*. 7: 100134.

Mukherjee et al., 2016 – *Mukherjee, A., Majumdar, S., Servin, A.D., Pagano, L., Dhankher, O.P., White, J.C.* (2016). Carbon nanomaterials in agriculture: a critical review. *Frontiers in Plant Science*. 7: 172.

Musuna-Garwe et al., 2018 – *Musuna-Garwe, C.C., Mukaratirwa-Muchanyereyi, N., Mupa, M., Mahamadi, C., Mujuru, M.* (2018). Preparation and characterization of nanocarbons from nicotiana tabacum stems. *AIMS Mater Sci*. 5: 1242-1254.

Naidu et al., 2023 – *Naidu, S., Pandey, J., Mishra, L.C., Chakraborty, A., Roy, A., Singh, I.K., Singh, A.* (2023). Silicon nanoparticles: Synthesis, uptake and their role in mitigation of biotic stress. *Ecotoxicology and Environmental Safety*. 255: 114783.

Narayanan, 2012 – *Narayanan, R.* (2012). Synthesis of green nanocatalysts and industrially important green reactions. *Green Chemistry Letters and Reviews*. 5(4): 707–725.

Nas, Ali, 2018 – *Nas, F.S., Ali, M.* (2018). The effect of lead on plants in terms of growing and biochemical parameters: a review. *MOJ Ecology & Environmental Sciences*. 3(4): 265-268.

Nath et al., 2023 – *Nath, P.C., Ojha, A., Debnath, S., Sharma, M., Sridhar, K., Nayak, P.K., Inbaraj, B.S.* (2023). Biogeneration of valuable nanomaterials from agro-wastes: A comprehensive review. *Agronomy*. 13(2): 561.

Neme, Mohammed, 2017 – *Neme, K., Mohammed, A.* (2017). Mycotoxin occurrence in grains and the role of postharvest management as mitigation strategies. A review. *Food Control*. 78: 412-425.

Nikolaev et al., 2023 – *Nikolaev, B., Yakovleva, L., Fedorov, V., Li, H., Gao, H., Shevtsov, M.* (2023). Nano-and microemulsions in biomedicine: From theory to practice. *Pharmaceutics*. 15(7): 1989.

Nizamuddin et al., 2019 – *Nizamuddin, S., Jadhav, A., Qureshi, S.S., Baloch, H.A., Siddiqui, M., Mubarak, N., Griffin, G., Madapusi, S., Tanksale, A., Ahamed, M.I.* (2019). Synthesis and characterization of polylactide/rice husk hydrochar composite. *Scientific Reports*. 9(1): 5445.

Pace, 2001 – *Pace, N.R.* (2001). The universal nature of biochemistry. *Proceedings of the National Academy of Sciences*. 98(3): 805-808.

Panas et al., 2014 – *Panas, A., Comouth, A., Saathoff, H., Leisner, T., Al-Rawi, M., Simon, M., Seemann, G., Dossel, O., Mulhopt, S., Paur, H.-R., et al.* (2014). Silica nanoparticles are less toxic to human lung cells when deposited at the air–liquid interface compared to conventional submerged exposure. *Beilstein Journal of Nanotechnology*. 5(1): 1590-1602.

Parmanik et al., 2022 – *Parmanik, A., Bose, A., Ghosh, B.* (2022). Research advancement on magnetic iron oxide nanoparticles and their potential biomedical applications. *Minerva Biotechnology & Biomolecular Research*. 34(2).

Qu et al., 2013 – *Qu, X., Brame, J., Li, Q., Alvarez, P.J.* (2013). Nanotechnology for a safe and sustainable water supply: enabling integrated water treatment and reuse. *Accounts of Chemical Research*. 46(3): 834-843.

Rajiv Gandhi et al., 2012 – *Rajiv Gandhi, R., Gowri, S., Suresh, J., Selvam, S., Sundrarajan, M*. (2012). Biosynthesis of tin oxide nanoparticles using corolla tube of *Nyctanthes arbor-tristis* flower extract. *Journal of Biobased Materials and Bioenergy*. 6(2): 204-208.

Rajput, 2015 – *Rajput, N.* (2015). Methods of preparation of nanoparticles-a review. *International Journal of Advances in Engineering & Technology*. 7(6): 1806.

Raman et al., 2017 – *Raman, S.M., Ismail, N.A., Jamari, S.S.* (2017). Preparation and characterization of impregnated commercial rice husks activated carbon with piperazine for carbon dioxide (CO2) capture. In: *IOP Conference Series: Materials Science and Engineering*. 206: 012005. IOP Publishing.

Ranaweera et al., 2017 – *Ranaweera, C., Kahol, P., Ghimire, M., Mishra, S., Gupta, R.K.* (2017). Orange-peel-derived carbon: designing sustainable and high-performance supercapacitor electrodes. *C*. 3(3): 25.

Rangaraj, Venkatachalam, 2017 – *Rangaraj, S., Venkatachalam, R*. (2017). A lucrative chemical processing of bamboo leaf biomass to synthesize biocompatible amorphous silica nanoparticles of biomedical importance. *Applied Nanoscience*. 7: 145-153.

Rasmussen et al., 2013 – *Rasmussen K, Mech A, Mast J, De Temmerman P, Waegeneers N, Van Steen F, Pizzolon J, De Temmerman L, Van Doren E, Jensen K, Birkedal R, Levin M, Nielsen S, Koponen I, Clausen P, Kembouche Y, Thieriet N, Spalla O, Giuot C, Rousset D, Witschger O, Bau S, Bianchi B, Shivachev B, Gilliland D, Pianella F, Ceccone G, Cotogno G, Rauscher H, Gibson P, Stamm H*. (2013). Synthetic Amorphous Silicon Dioxide (NM-200, NM-201, NM-202, NM-203, NM-204): Characterisation and Physico-Chemical Properties. EUR 26046. Luxembourg (Luxembourg): Publications Office of the European Union. JRC83506

Rokade et al., 2016 – *Rokade, A.A., Patil, M.P., Yoo, S.I., Lee, W.K., Park, S.S.* (2016). Pure green chemical approach for synthesis of Ag2O nanoparticles. *Green Chemistry Letters and Reviews*. 9(4): 216-222.

Rutgers New…, 2018 – Rutgers New Jersey Agricultural Experiment Station. Understanding Soil Microbes and Nutrient Recycling. 2018. [Electronic resource]. URL: https://njaes.rutgers.edu/fs1278

Saleh, Alaqad, 2016 – *Saleh, T., Alaqad, K.* (2016). Analytical toxicology gold and silver nanoparticles: Synthesis methods, characterization routes and applications towards drugs. *Journal of Environmental and Analytical Toxicology*. 6(4).

Sankar et al., 2016 – *Sankar, S., Sharma, S.K., Kaur, N., Lee, B., Kim, D.Y., Lee, S., Jung, H.* (2016). Bio- generated silica nanoparticles synthesized from sticky, red, and brown rice husk ashes by a chemical method. *Ceramics International*. 42(4): 4875-4885.

Selvakumari et al., 2017 – *Selvakumari, J.C., Ahila, M., Malligavathy, M., Padiyan, D.P.* (2017). Structural, morphological, and optical properties of tin(IV) oxide nanoparticles synthesized using *Camellia sinensis* extract: a green approach. *International Journal of Minerals, Metallurgy, and Materials*. 24: 1043-1051.

Seroka et al., 2022 – *Seroka, N.S., Taziwa, R.T., Khotseng, L. (2022)*. Extraction and synthesis of silicon nanoparticles (SiNPs) from sugarcane bagasse ash: a mini review. *Applied Sciences*. 12(5): 2310.

Sharar, Bozeya, 2017 – *Sharar, M., Bozeya, A.* (2017). Green Chem. Lett. Rev. 2017, 10: 3, 121; Naeimi, H., Babaei, Z. *Green Chem. Lett. Rev*. 10(3): 129.

Sharma et al., 2019 – *Sharma, G., Kumar, A., Sharma, S., Naushad, M., Dwivedi, R.P., ALOthman, Z.A., Mola, G.T.* (2019). Novel development of nanoparticles to bimetallic nanoparticles and their composites: A review. *Journal of King Saud University-Science*. 31(2): 257-269.

Sharma et al., 2020 – *Sharma, R., Jasrotia, K., Singh, N., Ghosh, P., Srivastava, S., Sharma, N.R., Singh, J., Kanwar, R., Kumar, A.* (2020). A comprehensive review on hydrothermal carbonization of biomass and its applications. *Chemistry Africa*. 3: 1-19.

Shinde et al., 2021 – *Shinde, P.S., Suryawanshi, P.S., Patil, K.K., Belekar, V.M., Sankpal, S.A., Delekar, S.D., Jadhav, S.A.* (2021). A brief overview of recent progress in porous silica as catalyst supports. *Journal of Composites Science*. 5(3). DOI: https://doi.org/10.3390/jcs5030075.

Singh et al., 2018 – *Singh, J., Kaur, N., Kaur, P., Kaur, S., Kaur, J., Kukkar, P., Kumar, V., Kukkar, D., Rawat, M.* (2018). Piper betle leaves mediated synthesis of biogenic SnO2 nanoparticles for photocatalytic degradation of reactive yellow 186 dye under direct sunlight. *Environmental Nanotechnology, Monitoring & Management*. 10: 331-338.

South Dakota..., 2024 – South Dakota State University Extension Why Carbon is So Important to Agriculture and Society. 2024. [Electronic resource]. URL: https://extension.sdstate.edu/why-carbon-so-important-agriculture-and-society (date of access: 15.07.2024).

Surattanamal et al., 2022 – *Surattanamal, F., Sulong, S., Waloh, N., Sohsansa, B., Dahlan, W., Suksuwan, A.* (2022). Physicochemical properties of cellulose extracted from hom thong banana peels. In: *Proceedings of The International Halal Science and Technology Conference*. 14: 194-201.

Szczyglewska et al., 2023 – *Szczyglewska, P., Feliczak-Guzik, A., Nowak, I.* (2023). Nanotechnology–general aspects: A chemical reduction approach to the synthesis of nanoparticles. *Molecules*. 28(13): 4932.

Taer et al., 2019 – *Taer, E., Apriwandi, A., Ningsih, Y., Taslim, R., et al.* (2019). Preparation of activated carbon electrode from pineapple crown waste for supercapacitor application. *International Journal of Electrochemical Science*. 14(3): 2462-2475.

Taer, Taslim, 2018 – *Taer, E., Taslim, R.* (2018). Brief review: Preparation techniques of biomass based activated carbon monolith electrode for supercapacitor applications. In: *AIP Conference Proceedings*. vol. 1927. AIP Publishing.

Thippeswamy et al., 2021 – *Thippeswamy, B.H., Maligi, A.S., Hegde, G.* (2021). Roadmap of effects of biowaste-synthesized carbon nanomaterials on carbon nano-reinforced composites. *Catalysts*. 11(12): 1485.

Van Bui et al., 2014 – *Van Bui, H., Nguyen, H.N., Hoang, N.N., Truong, T.T., Pham, V.B.* (2014). Optical and magnetic properties of Mn-doped ZnS nanoparticles synthesized by a hydrothermal method. *IEEE Transactions on Magnetics*. 50(6): 1-4.

Wang et al., 2018 – *Wang, G., Guo, Q., Chen, D., Liu, Z., Zheng, X., Xu, A., Yang, S., Ding, G.* (2018). Facile and highly effective synthesis of controllable lattice sulfur-doped graphene quantum dots via hydrothermal treatment of durian. *ACS Applied Materials & Interfaces*. 10(6): 5750–5759.

Wei et al., 2014 – *Wei, B., Hu, X., Li, H., Wu, C., Xu, X., Jin, Z., Tian, Y.* (2014). Effect of pHs on dispersity of maize starch nanocrystals in aqueous medium. *Food Hydrocolloids*. 36: 369-373.

Wibowo et al., 2015 – *Wibowo, D., Salamba, R., Nurdin, M., et al.* (2015). Preparation and characterization of activated carbon from coconut shell-doped TiO_2 in water solution. *Oriental Journal of Chemistry*. 31(4): 2337.

Wikipedia contributors..., 2024 – Wikipedia contributors: Agricultural waste (2024). Wikipedia, The Free Encyclopedia. 2024. [Electronic resource]. URL: https://en.wikipedia.org/wiki/Agriculturalwaste (date of access: 15.07.2024).

Yang, Park, 2019 – *Yang, G., Park, S.-J.* (2019). Conventional and microwave hydrothermal synthesis and application of functional materials: A review. *Materials*. 12(7): 1177.

Yearbook, 2013 – *Yearbook, F.S.* (2013). World food and agriculture. Food and Agriculture Organization of the United Nations, Rome 15.

Zhao et al., 2020 – *Zhao, X., Wei, C., Gai, Z., Yu, S., Ren, X.* (2020). Chemical vapor deposition and its application in surface modification of nanoparticles. *Chemical Papers*. 74: 767-778.

Zope et al., 2022 – *Zope, G., Goswami, A., Kulkarni, S.* (2022). Isolation and characterization of cellulose nanocrystals produced by acid hydrolysis from banana pseudostem. *BioNanoScience*. 12(2): 463-471.

Zuo et al., 2019 – *Zuo, K., Wu, J., Chen, S., Ji, X., Wu, W.* (2019). Superamphiphobic nanocellulose aerogels loaded with silica nanoparticles. *Cellulose*. 26(18): 9661-9671.

Published in the USA
Biogeosystem Technique
Issued since 2014.
E-ISSN: 2413-7316
2024. 11(2): 108-114

DOI: 10.13187/bgt.2024.2.108
https://bgt.cherkasgu.press

Mitigating the Negative Impacts of Caspian Sea Level Fluctuations On Coastal Infrastructure

Natalia V. Krupenina [a], Maksim Diuldin [b], Daniil S. Amelakhanov [a], Denis A. Egorov [a], Sergey E. Nikitin [c], Yury A. Nikolaev [c], Vasily Yu. Rud [a, c, *], Shoirbek A. Olimov [d], Yuri K. Smirnov [a], Sharifa Utamuradova [d], Daria A. Valiullina [e]

Paper Review Summary:
Received: 2024, November 30
Received in revised form: 2024, December 15
Acceptance: 2024, December 26

[a] Admiral Makarov State University of Maritime and Inland Shipping, Saint Petersburg, Russian Federation
[b] Peter The Great Saint-Petersburg Polytechnic University, Saint Petersburg, Russian Federation
[c] Ioffe Physico-Technical Institute, Saint Petersburg, Russian Federation
[d] Research Institute of Physics of Semiconductors and Microelectronics under the National University, Tashkent, Republic of Uzbekistan
[e] Kazan State Academy of Veterinary Medicine named after N.E. Bauman, Kazan, Russian Federation

Abstract

Natural fluctuations of the Caspian Sea level create many problems for its coastal infrastructure, complicate navigation and fishing, and negatively affect the ecological situation both in the coastal zone and in the coastal water area. It is necessary to deal with a complexity in a sea area alteration very carefully in order not to destroy the fragile ecological balance of coastal flora and fauna. To reduce the negative consequences of a northern water area shoaling of the Caspian Sea, a dredging is constantly carried out, which requires a careful planning due to a constant variability of the sea area boundaries. Taking into account this fact, the problem of permanent monitoring of newly formed closed water bodies with the help of autonomous water drones that allow to quickly build a 3d model of the water body for dredging planning becomes urgent. As a rule, such bodies of water are formed far from large settlements and energy sources, and the process of surveying the water body can stretch in time, so the problem of recharging the batteries of the drone becomes very relevant and is solved with the help of solar panels. The data received from the distance sensors can be noisy, so they are subjected to a de-noising procedure.

Keywords: Reducing the level of the Caspian Sea, maintaining shipping and fishing, maintaining the ecology of the coastal zone, dredging, Arduino robotics, autonomous water drones, recharging batteries with solar panels, cleaning received data from noise, volumetric model of a reservoir, freely distributed software.

* Corresponding author
E-mail addresses: ecobaltica@gmail.com (V.Yu. Rud)

1. Introduction

The Caspian Sea is essentially an isolated inland water body – a lake – and has no outflow to the World Ocean (Figure 1). This isolation and dependence on the volume of runoff from rivers flowing into it is a reason for significant fluctuations in its water level and, as a consequence, for environmental problems and problems in the operation of coastal infrastructure (Samant et al., 2023; Pörtner et al., 2022). If the water level drops significantly, shoals appear and impede navigation and fishing; if the water level rises, flooding of coastal areas becomes a problem (Prange et al., 2020; Hollis, 1978). Long-term water level fluctuation observation in the Caspian Sea demonstrates periodic long-term increase or decrease in a water level, which are a natural process that must be adapted to minimize the damage caused (Akbari et al., 2020; Pekel et al., 2016; Kislov et al., 2014; Efimov et al., 2015).

Fig. 1. Relief of the Caspian Sea area

The Northern Caspian Sea is a powerful navigable artery connecting the states on its shores with sea and river ports of the European part of Russia, a large volume of cargo operation is transported through its, therefore, maintaining the proper condition of waterways, including their sufficient depth, is of strategic importance for the whole country. In recent years, there has been a sharp drop in the level of the Caspian Sea, which leads to siltation and the formation of shoals and isolated water bodies in place of its former water surface, which greatly complicates the work of the shipping and fishing industries of the coastal territories (Grishanin, 1979; Shipulin, 2024; PRONauka, 2024; Samant, Prange, 2023; Demin, 2007).

Hydrological studies show that the main causes of the Caspian Sea shallowing are climate change and anthropogenic impact (Wang et al., 2018; Healy et al., 2007). While the global sea level is rising due to melting glaciers and expansion of warm water, the Caspian Sea, being a closed body of water with no outflow to the ocean, reacts to local climatic conditions (Koriche et al., 2021; Arpe et al., 2000). An increase in air temperature leads to an increase in evaporation, while a decrease in precipitation reduces the inflow of river water (Chen et al., 2017; Mischke, 2020). Reduced water surface area leads to degradation of coastal ecosystems, disappearance of marshes and deltas, which provide habitat for many species of birds and fish. Unique species, such as Caspian seal and sturgeons, are threatened by habitat reduction and changes in the food chain (Aliyev, 2024).

The regulation of river flow and the resulting drop in water levels in the Caspian Sea has led to changes in natural biogeochemical cycles (Berkeliev, 2024).

Massive hydro construction on the Volga and then on other rivers of the Caspian basin has deprived Caspian sturgeons of most of their natural spawning grounds. Fish passage structures at the dams suffer from many technical deficiencies, and the system of counting spawning fish is also far from perfect. However, with the best systems, the juvenile fish rolling down the river will not return to the sea, but will form artificial populations in polluted and food-poor reservoirs. It was dams, not water pollution and not overfishing, that were the main reason for the reduction of the sturgeon herd. Meanwhile, the construction of dams has caused even greater problems. The Northern Caspian was once the richest part of the sea. Here, the Volga brought mineral phosphorus (about 80 % of the total input), providing the bulk of primary biological (photosynthetic) production. As a consequence, 70 % of sturgeon stocks were formed in this part of the sea. Now most of the phosphate is consumed in the Volga reservoirs, and phosphorus enters the sea in the form of living and dead organic matter. As a result, the biological cycle has changed radically.

The Ural remains the only unregulated major river in the Caspian basin, but the condition of spawning grounds on this river is also very unfavorable. The main problem today is siltation of the riverbed. The soils in the Ural valley were once protected by forests; later these forests were cut down and the floodplain was plowed almost to the water's edge. After “for the purpose of sturgeon conservation”, navigation was stopped on the Ural River, work on cleaning the fairway ceased, making most of the spawning grounds on this river inaccessible.

Active dredging to facilitate the movement of water masses to the main sea area can mitigate the negative effects of these phenomena. Dredging can be initiated after monitoring the boundaries and depths of the resulting isolated water bodies. Dredging is continuously carried out to control siltation and sedimentation, thus reducing the length of one-way traffic areas and constructing protection structures against siltation and shallowing. To survey such areas, autonomous water drones can be used, which will operate under the control of a program loaded in them and transmit information to a stationary computer that forms a 3d-model of the geometry and depths of the water body. In order to predict the occurrence of difficult areas and design dredging works, it is necessary to continuously monitor channel processes and calculate sediment loadings.

This work is devoted to predicting and mitigating environmental, shipping and fishing problems in the coastal areas of the Northern Caspian Sea, which arise due to its level lowering.

Formally, the task can be formulated as follows: to create a robotic solution that can move on the surface of a reservoir, create its 3D model and track its position in real time.

2. Materials and methods

To solve the presented task, we use Arduino controller and compatible sensors. Robotics compatible with Arduino controller has good technical parameters and there is a free software Arduino IDE. Arduino controllers are quite budget-friendly compared to their counterparts: Teensy, Particle Photon, BeagleBone.

We use Arduino Uno as a main controller board (Figure 2). The controller is equipped with an ATmega328 microcontroller and operates at 5 volts. It has 14 digital I/O, of which 6 support PWM, and 6 analog inputs. The maximum current from a single I/O pin is 40 milliamps. Flash memory has a capacity of 32 kilobytes. RAM is two kilobytes and EEPROM is one kilobyte. The controller clock frequency is 016 megahertz. The board has dimensions of 69×53 mm and is equipped with a USB-type A-B connector.

The robot must be able to move on the water surface while maintaining stability and minimizing oscillations. The robot body will be made of foam for good buoyancy. To prevent rollovers, we will use the MPU-6050 gyroscope and accelerometer sensor. The sensor has small dimensions of 21×16×3 mm, weighs about 10 g, operates at 6 VDC consuming 350 mA. Gyroscope range is ± 250; 500; 1000; 2000 °/s, accelerometer range is ± 2; 4; 8; 16 g.

The robot moves with the help of two motors with screws. The motor dimension of 70×22×18 mm is small, weigh is about 50 g, it operates at a voltage of 6 v, consuming up to 500 mA. And as a rotary mechanism we will use a servo drive, it will direct the propellers in the desired direction. The MG946R servo drive has small dimensions of 43×40.7×19.7 mm, weighs 55 g, operates at a 4.8-7.2 VDC consuming up to 1.2 A.

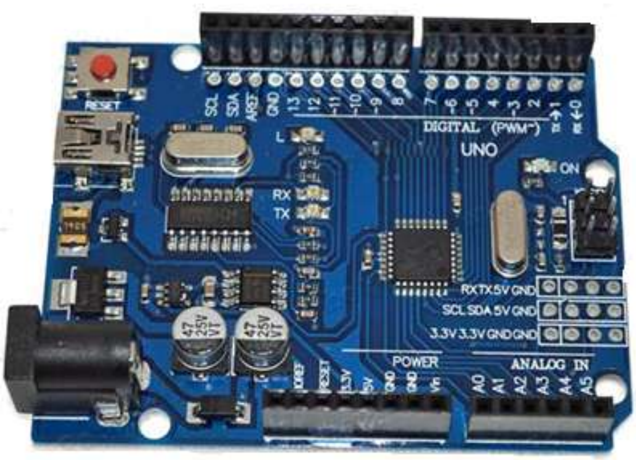

Fig. 2. Arduino Uno board

The system must be able to collect data on a depth and a shape of the bottom as well as the contours of the tank walls. A waterproof ultrasonic sensor JSN-SR04T is suitable for a depth measurement. The sensor has small dimensions of 41×28.5×28.5 mm, weighs about 8 g, operates at a voltage of 5 VDC, consumes 5 mA, ultrasonic frequency of 40 kHz, measured range up to 4.5 m with an accuracy of 0.003 m. We use the HC-SR04 ultrasonic sensor to recognize the boundaries of the tank. The sensor also has small dimensions of 45×20×15 mm, weighs about 10 g, operates at a voltage of 5 VDC, during standby consumes 2 mA, during measurement consumes up to 15 mA, ultrasonic frequency of 40 kHz, measured range up to 4 m with an accuracy of 0.003 m. A 3D model will be created from the received data. For data transmission we use Bluetooth sensor HC-06. The sensor has small dimensions 27×13×2.2 mm, weighs about 15 g, operates at a voltage of 3.3-5 VDC, consumes 50 mA, the range is up to 10 m.

The robot must track its location in the tank and transmit it in real time. For this task, we use a GPS sensor. The sensor has dimensions of 21×16×3 mm, weighs about 18 g, operates at a 4.4 VDC, consumes 45 mA, and has a location update rate of 5 Hz. The robot will be powered by two LiitoKala inr18650 batteries with a capacity of 2500 mA-h and a voltage of 3.7 VDC.

The water bodies formed as a result of the retreat of the Caspian Sea water area may have different geometric dimensions and depth, which will require their long-term survey, may be located at a considerable distance from the established coastline, where the infrastructure for recharging batteries is located, so in addition to providing the possibility of recharging them from the power-bank, it is still useful to provide for the possibility of using solar energy to ensure the operation of the robot through autonomous power supply. The most efficient use of the solar panel can be achieved by using an Arduino board that tracks the location of the sun (following the sun) in order to maximize the amount of energy generated by the solar panel (since it will always be turned towards the light) (Bard et al., 2000). The components required are Arduino Uno board, sg90 servo motor, solar panel, photoresistor (2 pcs), 10k ohm resistor (2 pcs), battery. Here the photoresistor will work as light detector and when light starts falling on the photoresistor, its resistance decreases, that's why the photoresistors are often used in various light or darkness detectors.

Two photoresistors are placed at the both ends of the solar panel and a servo motor is used to rotate the solar panel. The servo motor rotates the solar panel towards the photoresistor whose resistance is lower, which means that more sunlight is falling on it. If the same amount of sunlight falls on both photoresistors, the servo motor does not work and does not turn the solar panel. So the servo motor will try to rotate the solar panel to a position where both photoresistors have approximately the same resistance, which would mean that they receive approximately the same amount of sunlight. If the resistance of one photoresistor becomes less than that of the other, then the servo motor will rotate the solar panel in the direction of that photoresistor. In this solar panel following the sun design, the Arduino board is powered by a 9 VDC battery and the rest of the circuit is powered by the Arduino. The recommended voltage for powering the Arduino board is between 7 and 12 VDC (although you can actually supply between 6 and 20 VDC), so our 9 VDC is well within the recommended range.

If the solar panel is rotated to follow the sun, the efficiency of its operation will be higher than if it just stays in a stable position. However, a correction should not be done too often, so that the increase in efficiency is not reset by the corrector motors.

The market of microcontrollers offers various variants of solar panels for Arduino-products, which can be used both jointly and separately. Besides, it is possible to assemble an angular battery from the panels, and if you fold it in a triangle, part of the panels will "look" to the east, part – to the south, part – to the west. So that it will not be necessary to rotate the battery, and all the power of solar energy will be used not to solve auxiliary problems, but to solve the main task.

The data obtained from the sensors are collected and accumulated in real time in the database of Blender 3D package – a freely distributed software package for creating 3D computer graphics, which are used for 3D modeling and visualization in various spheres of activity.

When receiving a digital signal from sensors, the problem of its purification, i.e. separation of the active signal from noise, is acute. A signal received from the sensors always comes with noise, and it is important to be able to filter it properly. Good quality noise filtering can reduce the error and increase the quality of the sensor measurement.

Two types of noise are commonly attempted (Figure 3):

– Constant noise (additive white Gaussian noise) with relatively stable amplitude and

– Random pulses caused by external factors.

The noise amplitude is the standard deviation of the noisy signal from the unnoisy signal.

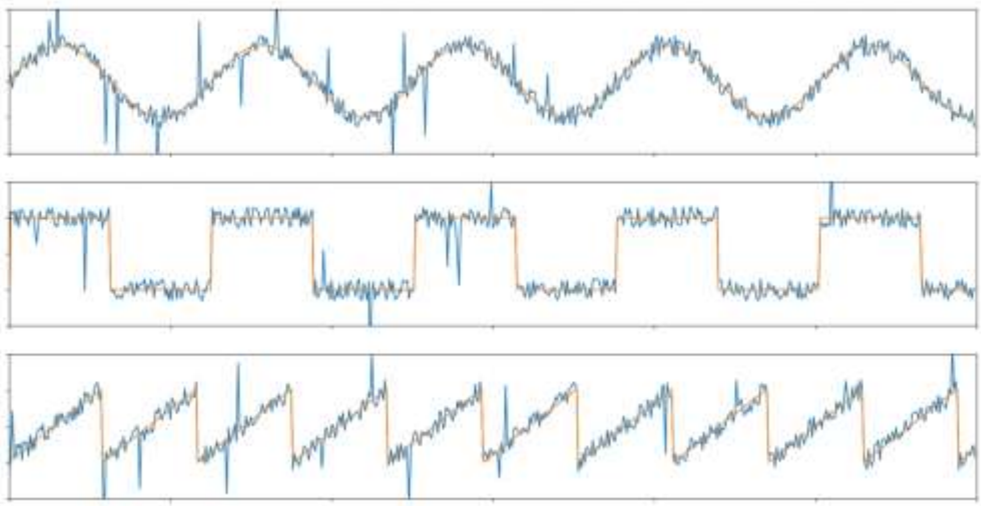

Fig. 3. Cleaning a noisy signal

The simplest filtering method is to filter the graph using the arithmetic mean method (Bukhtiyarov, 2021). The algorithm of this method is quite simple – it will require a buffer of several previous values, each time a sensor is polled, the buffer will be shifted (the first element is removed and the new sensor value is added to the end). The size of the buffer will determine the result and the speed of the code. The algorithm does very well with filtering, but its problem is the loss of performance because the controller has to do a lot of floating point calculations, which can affect the speed of code execution. If the sensor is not polled very often, this method copes with the task perfectly well, the main thing is to have a fixed buffer size.

With random impulses the median filter copes well, which is easy to implement and in combination with the arithmetic mean method gives quite a decent result.

To create a 3D model, we will use the free publicly available software Blender. Indicators from sensors will be converted into coordinates and written to obj file using the following libraries: FS.h and LittleFS.h. The FS.h library is needed to process the file, and LittleFS.h is needed to create and access the file system. Then, if we open the file, we can see a model of the tank.

Initially, the robot is placed on the edge of the tank and moves a short distance away from it (15-20 cm to be able to turn without touching the edge of the tank). The robot should walk around the edge of the tank at a short distance from the edge, collecting route coordinates and measured depths while building a 3D model of the tank edges. After that, the entire surface of the reservoir should be explored using the uniform grid method, instantiating the depths of the reservoir in the 3D model. The robot's movement can then be controlled from the remote control, displaying the route of its movement in the 3D model.

3. Results and discussion

As a result of the performed research, the project of a robot – an aquatic drone, which performs the survey of water bodies newly formed during the retreat of the Caspian Sea water area, was built. The robot examines the geometry of the water body banks and its depth, promptly transmits the information to the associated computer, which cleans the noise data and builds a volumetric model of the water body in a free 3D-modeling package, and allows to build a dredging plan. The robot's design includes the use of solar panels to recharge the robot when conducting long-term studies.

4. Conclusion and recommendations

The proposed robot project for monitoring of newly formed compact water bodies in the place of the former Caspian Sea water area when its level decreases will allow building a dredging project to ensure the necessary conditions for navigation and fishery.

References

Samantet, Prange, 2023 – *Samant, R., Prange, M.* (2023). Climate-driven 21st century Caspian Sea level decline estimated from CMIP6 projections. *Commun Earth Environ* 4: 357. DOI: https://doi.org/10.1038/s43247-023-01017-8

Pörtner et al., 2022 – *Pörtner, H.-O. et al.* (2022). Climate change 2022: Impacts, adaptation and vulnerability. *In IPCC Sixth Assessment Report* (IPCC).

Prange et al., 2020 – *Prange, M., Wilke, T., Wesselingh, F.P.* (2020). The other side of sea level change. *Commun. Earth Environ.* 1: 1-4.

Hollis, 1978 – *Hollis, G.* (1978). The falling levels of the Caspian and Aral Seas. *Geogr. J.* 144: 62-80.

Akbari et al., 2020 – *Akbari, M. et al.* (2020). Vulnerability of the Caspian Sea shoreline to changes in hydrology and climate. *Environ. Res. Lett.* 15: 115002.

Pekel et al., 2016 – *Pekel, J.-F., Cottam, A., Gorelick, N., Belward, A.S.* (2016). High-resolution mapping of global surface water and its long-term changes. *Nature*. 540: 418-422.

Kislov et al., 2014 – *Kislov, A., Panin, A., Toropov, P.* (2014). Current status and palaeostages of the Caspian Sea as a potential evaluation tool for climate model simulations. *Quat. Int.* 345: 48-55.

Efimov et al., 2015 – *Efimov, V., Volodin, E., Anisimov, A., Barabanov, V.* (2015). Regional projections of climate change for the Black Sea–Caspian Sea area in late 21st century. *Phys. Oceanogr.* 49: 66.

Grishanin, 1979 – *Grishanin, K.V.* (1979). Dynamics of riverbed flows. *Leningrad: Hydrometeoizdat*. 312 p.

Shipulin, 2024 – *Shipulin, S.* (2024). The level of the Caspian Sea may decrease by another 1 m in the next 10 years. [Electronic resource]. URL: https://nauka.tass.ru/nauka/21706433 (date of access: 29.11.2024).

PRONauka, 2024 – PRONauka. Scientists warned about the risks to navigation due to the shallowing of the Caspian Sea. 2024. [Electronic resource]. URL: https://kavkaz.rbc.ru/kavkaz/freenews/66ed66259a794768ceefb707 (date of access: 29.11.2024)

Demin, 2007 – *Demin, A.* (2007). Present-day changes in water consumption in the Caspian Sea basin. *Water Res.* 34: 237-253.

Wang et al., 2018 – *Wang, J. et al.* (2018). Recent global decline in endorheic basin water storages. *Nat. Geosci.* 11: 926-932.

Healy et al., 2007 – *Healy, R.W., Winter, T.C., LaBaugh, J.W., Franke, O.L.* (2007). Water Budgets: Foundations for Effective Water-Resources and Environmental Management (*US Geological Survey Reston*, Virginia).

Koriche et al., 2021 – *Koriche, S.A., Singarayer, J.S. Cloke, H.L.* (2021). The fate of the Caspian Sea under projected climate change and water extraction during the 21st century. *Environ. Res. Lett*. 16: 094024.

Arpe et al., 2000 – *Arpe, K. et al.* (2000). Connection between Caspian Sea level variability and ENSO. *Geophys. Res. Lett*. 27: 2693-2696.

Chen et al., 2017 – *Chen, J. et al.* (2017). Long-term Caspian Sea level change. Geophys. *Res. Lett*. 44: 6993-7001.

Mischke, 2020 – Mischke, S. (2020). Large Asian Lakes in a Changing World: Natural State and Human Impact. Natural State and Human Impact.

Aliyev, 2024 – *Aliyev, T.* (2024). What is the threat to the ecology and economy of the shallowing of the Caspian Sea. [Electronic resource]. URL: https://rg.ru/2024/10/22/reg-skfo/minus-tri-metra-za-30-let.html (date of access: 29.11.2024).

Berkeliev, 2024 – *Berkeliev, T.* (2024). The main environmental problems of the Caspian Sea. https://www.biodiversity.ru/programs/seal/publications/soes20020709.html (date of access: 29.11.2024).

Bard et al., 2000 – *Bard, E., Raisbeck, G., Yiou, F., Jouzel, J.* (2000). Solar irradiance during the last 1200 years based on cosmogenic nuclides, *Tellus*, 52B: 985-992.

Bukhtiyarov, 2021 – *Bukhtiyarov, M.* (2024). Signal noise filtering. [Electronic resource]. URL: https://habr.com/ru/articles/588270 (date of access: 29.11.2024).

Published in the USA
Biogeosystem Technique
Issued since 2014.
E-ISSN: 2413-7316
2024. 11(2): 115-123

DOI: 10.13187/bgt.2024.2.115
https://bgt.cherkasgu.press

Features of the Study of Biofouling on Ship Hulls Using Modern Possibilities of Artificial Intelligence

Vsevolod V. Kirgizov [a], Maksim Diuldin [b], Natalia V. Krupenina [a], Shoirbek A. Olimov [c], Vasiliy Yu. Rud [a, d, *], Sharifa Utamuradova [c], Lenar R. Valiullin [e]

[a] State University of Maritime and Inland Shipping named after Adm. S.O. Makarov, Saint-Petersburg, Russian Federation
[b] Peter The Great Saint-Petersburg Polytechnic University, Saint-Petersburg, Russian Federation
[c] Research Institute of Physics of Semiconductors and Microelectronics under the National University, Tashkent city, Republic of Uzbekistan
[d] Ioffe Physico-Technical Institute, Saint-Petersburg, Russian Federation
[e] Federal Center for Toxicological, Radiation and Biological Safety, Kazan, Russian Federation

Paper Review Summary:
Received: 2024, November 29
Received in revised form: 2024, December 18
Acceptance: 2024, December 26

Abstract

The study of biofouling on ship hulls has emerged as a critical area of research due to its significant impact on maritime operations and vessel longevity. This article presents a comprehensive overview of the current state of biofouling, emphasizing its detrimental effects on corrosion processes affecting ship structures. Biofouling not only accelerates corrosion but also increases fuel consumption, thereby raising operational costs and contributing to environmental concerns. The article delves into the intricate structure of biofouling, exploring the various organisms involved and their interactions with the hull materials.

Furthermore, the application of artificial intelligence (AI) in underwater drones for biofouling removal is discussed in detail. A classification of underwater drones specifically designed for this purpose is provided, alongside a schematic representation of their construction. This section highlights the technological advancements that enable drones to autonomously detect and mitigate biofouling, showcasing the integration of AI algorithms for enhanced performance.

Additionally, the article describes the design of a cleaning device attached to the drone, detailing its operational mechanisms and effectiveness in biofouling removal. A brief overview of the drone's control system is also included, illustrating how AI facilitates precise navigation and task execution. This research underscores the potential of modern AI technologies in revolutionizing the management of biofouling, ultimately contributing to more sustainable maritime practices and improved vessel maintenance strategies.

Keywords: biofouling, speed, plant, drones, artificial intelligence

[*] Corresponding author
E-mail addresses: rudvas.spb@gmail.com (V.Yu. Rud)

1. Introduction

In order to solve the issues of intensification of sea freight and passenger transportation in recent times, especially with the increasing role of shipping along the Northern Sea Route, there is an increasing need to take into account many factors that have not been given due attention before (Orlova, Rodionov, 2020; Zvyagintsev, 2005). They require non-standard approaches, construction of complex models, and conducting various studies that often lie at the junction of many different sciences (Zvyagintsev, Moshchenko, 2002). One of such tasks seems to us to be the study of the problem of biofouling on the surface of ships. Problems that previously, in principle, used different approaches (Ovchinnikov et al., 1974; Schansker et al., 2003). However, it was not possible to build a complete picture of the model of formation of these formations on the hulls of ships, at a time when such reasons lead to the emergence of problems with the loss of speed of ships (Bixler, Bhushan, 2012; Lenbaum et al., 2015).

If we consider the chain of problems, the formation of biofouling for a vessel leads to a decrease in its shipping characteristics and, first of all, to a decrease in its so-called cruising speed. When a vessel's speed drops, it becomes necessary to increase its operating costs, which means an increase in engine power and fuel costs and an increase in the financial costs of ship operators (Orlova, Rodionov, 2020).

2. Results and discussion

Status of the issue

Work on attempts to solve this problem has been going on for quite some time (Lazar, Schansker, 2009; Schansker et al., 2003; Joliot P., Joliot A., 2005). They are trying to develop new and new approaches and technologies to reduce biofouling, new methods to remove these growths from the surface of a vessel (Miyake et al., 2005). However, solving these issues opens up new and new questions, including environmental ones, because uncontrolled removal of bio-growths can bring to us microorganisms and algae that have migrated from other world regions. Which in turn can significantly reformat the biodiversity of domestic waters (Albitar et al., 2013; 2014; 2016; Aldrich, Qi, 2005).

Thus, the main objective of the study was to work out issues related to the mechanisms of biofouling formation, to study methods of diagnostics and combating this phenomenon, to understand which issues remain less studied and what can be done in this direction using the methods and techniques at the disposal of researchers (Asbeck et al., 2006; Balashov et al., 2011). The tasks for the study were literary studies of issues related to the emergence and development of biofouling of ships, the study of their biological composition, the processes of modeling their formation, methods of counteraction, the use of modern digital methods and techniques (Bax et al., 2003; Bixler, Bhushan, 2012).

Biofouling and corrosion

So, it is worth recognizing that biofouling is a very interesting form of biological symbiosis of plant and animal life forms - a set of attached and mobile forms of organisms inhabiting anthropogenic surfaces in operation (Zvyagintsev, 2005; Zvyagintsev, Moshchenko, 2002). The importance of the issue is also determined by the fact that these same reasons lead to the loss of functionality of not only ships, but also parts of locks and port facilities (Caduff, 1990). These reasons sooner or later lead to corrosion (Chambers et al., 2006).

A study of the literature has made it possible to understand that, depending on the operating conditions and the state of the anti-corrosion protection means, the corrosion rate of the underwater part of the ship's hull, generally speaking, can vary within wide limits (Chen et al., 2010; 2012; 2017; Courson, Shelburne, 2001). In known cases of hull electro corrosion under the influence of stray currents, corrosion damage can develop at a rate of up to 5 mm/year. In the underwater part of the hull, the most intense corrosion damage can usually be observed in the area of the bow and stern counter as a result of the action of strong water jets causing mechanical destruction of the protective coating and the ship's hull, and on the hull, rudders and sternpost under the influence of the galvanic pair - hull – propeller (Cioanta, McGhin, 2017; Daltorio et al., 2005). As a result, it is necessary to frequently repair the nozzle or use means of its protection that exclude the use of paint and varnish coatings (Davidson et al., 2008). On the outside, the nozzle is painted with abrasion-resistant, non-swelling paints, on which an antifouling paint is also applied on top (Drake, Lodge, 2007).

Various types of fairings located in the underwater part of the hull are used in conditions typical for the part of the hull where they are located. The frontal areas of the fairing surface experience a more significant effect of water (Erneland, 2014). Therefore, the destruction of the protective coating, fouling and corrosion are most intense here (Ferreira et al., 2013). On ships sailing in the seas, freshwater basins and rivers of the tropics throughout the year, in the rest – in the warm season, fouling – various types of animals and algae settle on the underwater part of the hull, fairings, nozzles, rudders, mortars, brackets, as well as in the area of variable waterline (Floerl et al., 2010). Having settled and quickly multiplied, they not only make the underwater part rough, which reduces the speed of the vessel, but also destroy the protective coating. Inspection of the underwater part of the hull of operating ships and all structures located on it is possible when the vessel is docked or with the help of a diver (Holappa et al., 2013). A diver cannot always detect paint defects, correctly assess the danger of emerging signs of biofouling or corrosion damage and promptly eliminate them. Therefore, when defects in the protective coating and accompanying corrosion damage are detected, the vessel must be brought into the dock, which is associated with large material costs (Godwin, 2003). As a result, special attention must be paid to the quality of preparatory work, the choice of impact schemes and control technology.

The mechanism of fouling on marine or freshwater vessels and structures is based on biofilms that form on such structures, which are the link between marine or aquatic organisms and the structure itself (Holappa et al., 2013). Biofilms form and fouling organisms attach to all subsurface structures such as propellers, rudders, inlets and outlets, sonar housings and protective grilles, as shown in the Figure 1 the most common methods used to remove biofouling (Bixler, Bhushan, 2012) are dry dock cleaning, antifouling paint and periodic underwater cleaning. It was noted that a good method for removing biofouling is the use of high-pressure abrasives in dry docks. In the dry dock cleaning method, ship owners accept increased sailing costs and wait for the complete cleaning and repainting of the hull in the dock. The method requires the ship to enter the dock and completely leave the water, and then clean the surface of the vessel with high-intensity labor (Hopkins et al., 2009). Dry dock cleaning apparently has its drawbacks in the form of long work cycles, high labor intensity and high cleaning costs. In the antifouling paint method, the hulls of ships are coated with a soft antifouling paint that can effectively kill or inhibit the growth of organisms.

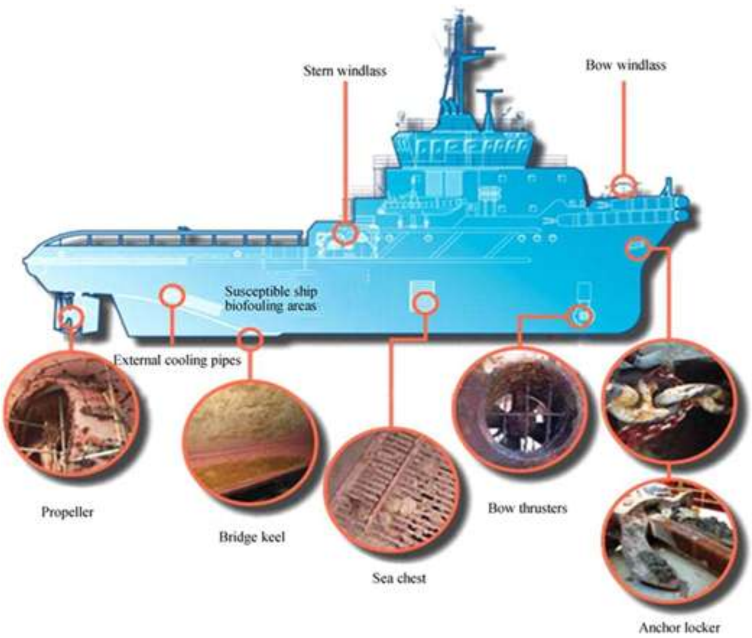

Fig. 1. Scheme of attachment of marine fouling organisms to the subsurface structures of the vessel

It is extremely important to know the structure of biofouling layers on a vessel, as can be seen from our research. At least in order to effectively combat biofouling. Moreover, in recent years, the most modern methods based on ultrasound and laser radiation have been effectively included in the number of methods (Hua et al., 2018; Huang et al., 2017). Therefore, it is important to develop the direction of biofouling diagnostics.

In general, it is accepted to consider that biofoulings are classified by the type of organisms, for example, simple organisms, which include algae and bacteria, as well as living organisms – mollusks, worms, small fish. Also interesting is the division by the degree of growth – biofilms and colonial organisms.

Study of the structure of biofouling

We attempted to study plants to understand the possibility of their identification in the same layer of biofouling material. We conducted such a study of photoluminescence on green plants and algae. In the experiment, it was found that plants, when excited by radiation with the excitation energies specified above, show bright red photoluminescence. The photoluminescence spectra for green plants in all cases are two closely spaced bands (Zvyagintsev, Moshchenko, 2002). It is important to note that the energies of both bands for different types of plants were almost the same (Orlova, Rodionov, 2020). We believe that modern technologies, such as underwater drones equipped with high-resolution cameras or mobile photoluminescence installations, provide unique opportunities for monitoring the condition of ship hulls in real time (Lenbaum et al., 2015). Using images obtained from such drones, deep learning algorithms are able to effectively process large arrays of visual data. These algorithms, based on neural networks, allow identifying and classifying different types of biofouling by learning from pre-labeled data (Kostenko et al., 2019). Transformational models such as convolutional neural networks (CNNs) show particularly high performance in visual classification tasks because they can extract meaningful features from images, making the identification process more accurate.

Involvement of artificial intelligence and the use of drones

One of the most promising areas of using artificial intelligence (AI) to classify biofouling is the use of real-time data transmission tools. Equipping underwater drones with an image transmission system allows monitoring the condition of the hull of ships or lock components directly during their operation. AI algorithms can be integrated into technical tools, analyzing incoming data and providing recommendations for necessary actions. Thus, ship owners can quickly respond to changes in the condition of the hull and carry out preventive or cleaning work in a timely manner, which in turn helps reduce operating costs and improves the efficiency of shipping.

However, for the successful implementation of such systems, it is important to consider a number of factors, such as the quality and availability of training data. The development of extensive and diverse datasets of biofouling images, as well as the implementation of data augmentation methods, can significantly improve the quality of classification (Kostenko et al., 2019). It is also important to consider the impact of different lighting conditions and underwater environments on the accuracy of the algorithms. Certification-based evaluation and testing systems can help assess the effectiveness of the developed solutions and ensure their reliability during operation.

In recent years, with the rapid development of robotics and artificial intelligence, hull cleaning robots have gradually become the focus of attention in this field – Figure 2 (Lee et al., 2022; Mazue et al., 2021). They can effectively and safely complete cleaning tasks in various water conditions, and have great economic and social value (Legg et al., 2015).

The underwater hull cleaning robot mainly consists of surface equipment and underwater equipment (Kalumuck et al., 1997). The surface equipment includes control, casting and retrieving units, and the underwater equipment includes slave industrial computer, adsorption mechanism, drive mechanism, cleaning mechanism, position sensors, orientation sensor, underwater camera, etc (Longo, Muscato, 2006; Mazue et al., 2011). The diagram of the underwater hull cleaning robot is shown in Figure 3.

The movement of the robot on the outside of the body is carried out by the motor, and its deviation is carried out by the difference in the angular velocity of the two motors. It uses a permanent magnet in adsorption. The brushes work during the movement along the specified route. The cleaning equipment consists of brushes, an actuator module of the drive and a support. The two motors that drive the two brushes rotate in opposite directions. The robot cleans while moving until the cleaning is completed (Menon et al., 2004).

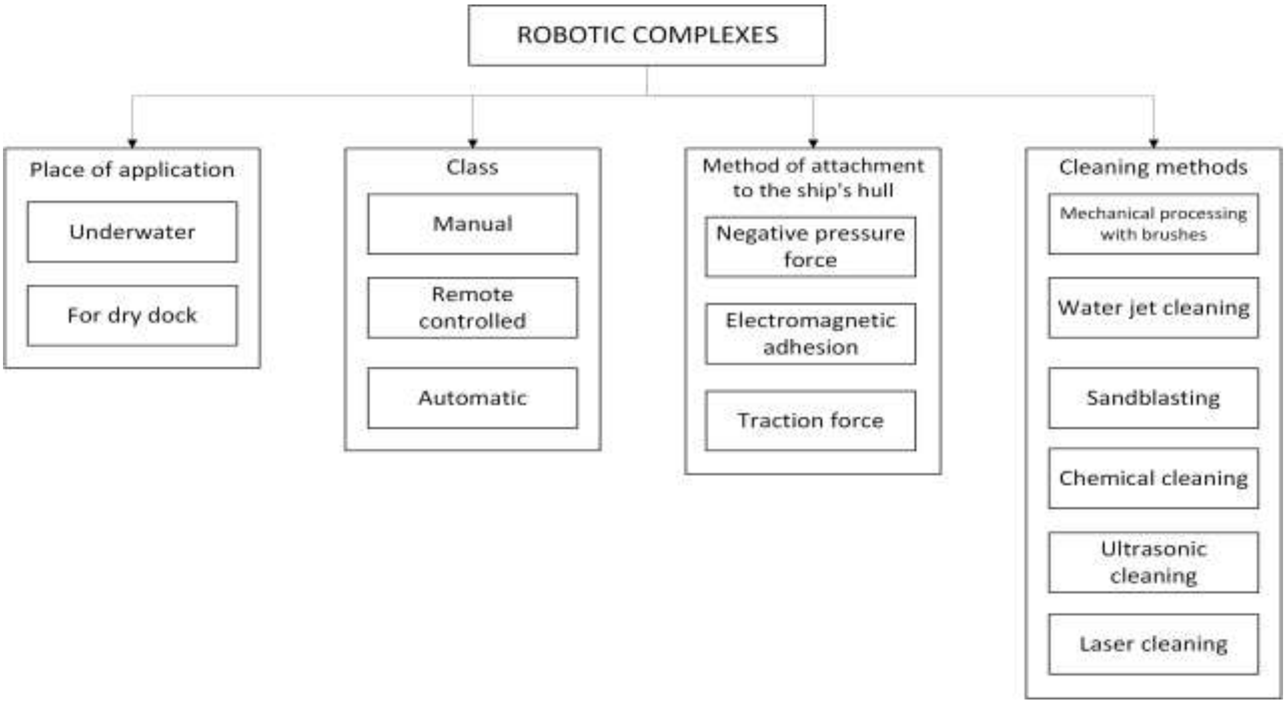

Fig. 2. Classification of robotic systems used for cleaning ship hulls from biofouling

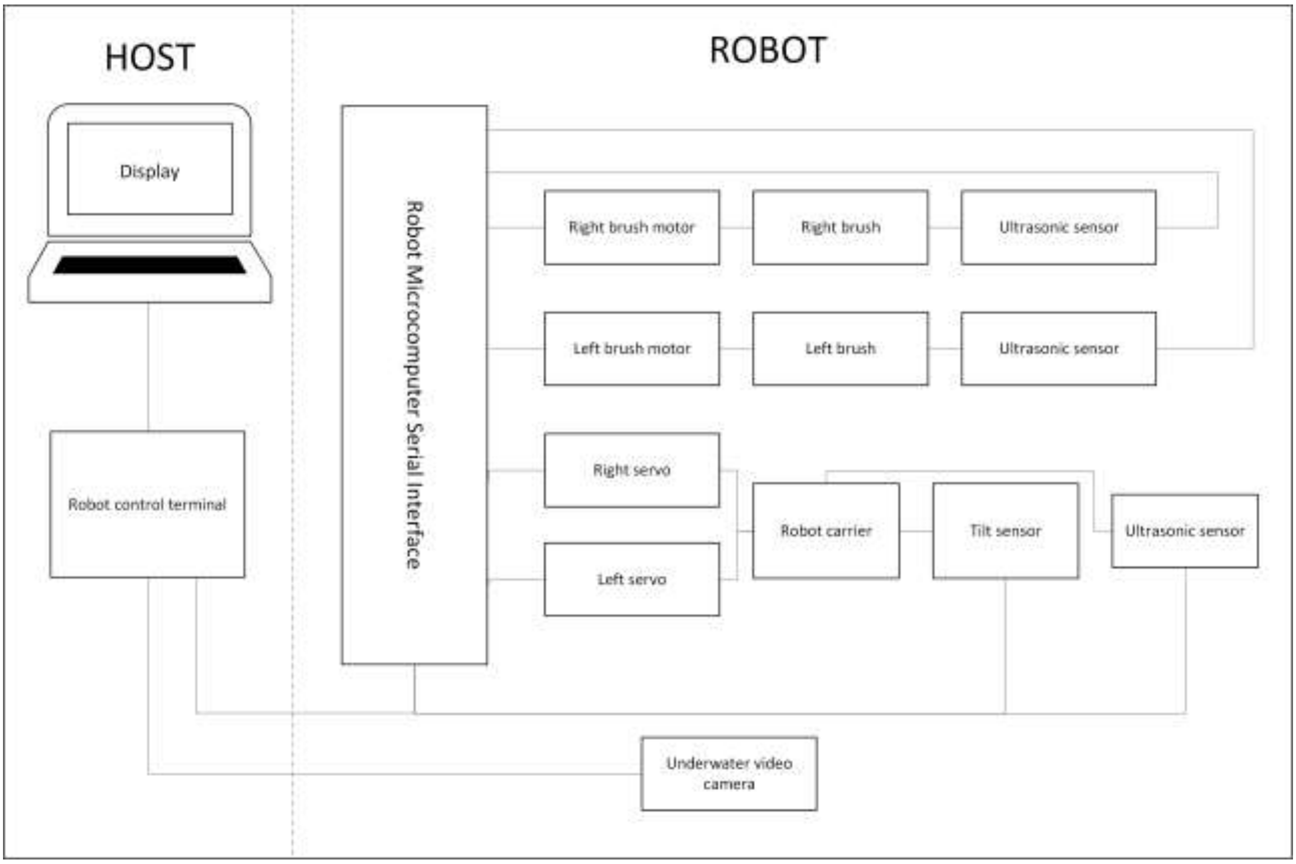

Fig. 3. Robot diagram

The underwater drone's workflow for inspecting and cleaning ship hulls from biofouling begins with its descent underwater, where it inspects the ship's hull or specific parts of it, such as the bottom and side. To obtain high-quality images of the propeller group (propulsor), it is necessary to stop the vessel, which avoids vibrations and allows the drone to record high-quality, high-resolution images. Once the full hull inspection is complete, the convolutional neural network analyzes the images obtained, finds and classifies biofouling based on pre-trained data (Morrisey, Woods, 2015). A decision is then made on the type of drone and the corresponding cleaning equipment required to effectively remove the identified type of biofouling as (Figure 4; Hua et al., 2018). In particular, it is recommended to use a drone that can attach to the ship's hull using the low-pressure method, which ensures reliable fixation and maneuverability in the underwater environment (Kostenko et al., 2019). This method is also preferable, since magnetization is prohibited on military ships, making it not a universal solution.

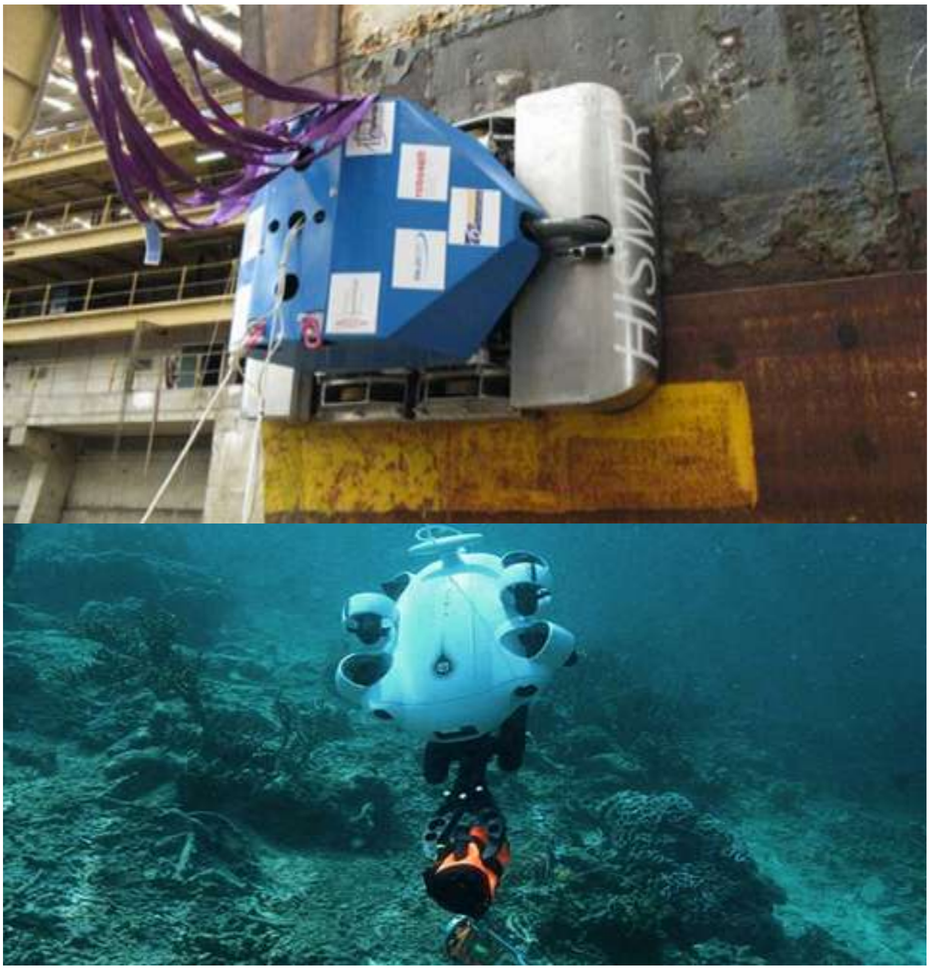

Fig. 4. An example of drones operating in dry dock and underwater mode to combat biofouling

Construction of underwater cleaning device

The underwater cleaning device is the drive of the underwater robot body cleaner. It consists of brushes, a power actuator (motor) and a support (Murphy et al., 2006). The cleaning tray, a stainless-steel half-coupling and a metal brush wire, which is also made of stainless steel, make up the brushes. To achieve high cleaning efficiency, a steel brush wire with good hardness and elasticity should be selected (Nassiraei et al., 2012). The cleaning tray is made of aluminum alloy and is fixed on its coupling, which is connected to the drive motor. The support is made of aluminum alloy, and the bearing is waterproof. Two cleaning devices are installed in the front part of the robot carrier, which rotates in the opposite direction.

Development of a management system

The control system of the underwater hull cleaning robot adopts two-level control (Oliveira, 2017). The main computer, which is placed in the container and moves on the deck, can perform human-machine interface interaction, input of the initial values of the environment, designation of the task, path planning and display of the robot information, etc. The slave computer is fixed on the carder of the robot, receives instructions from the main computer, controlling the task of moving the structure and cleaning unit. Information and power are transmitted through the umbilical cable. The position and gesture are determined by the inclinometer and the ultrasonic sensor, which controls and plans the task of the brushes. The underwater camera displays the information of the robot, and also checks the underwater hull of the vessel.

3. Conclusion

It is found that understanding the type of biofouling on the hull of a ship plays an important role in developing effective diagnostic and control methods. The application of AI to classify biofouling on ship hulls using images obtained by underwater drones is a promising area to help optimize operations in the maritime industry.

The proposed AI-powered drone scheme can be very effective, as it creates an efficient scheme of operation where underwater drones not only inspect but also help maintain the cleanliness and safe operation of vessels, providing a high degree of automation and minimizing human intervention.

This will improve the efficiency and timeliness of actions to prevent and remove biofouling, which, in turn, will help to increase the service life of the vessel and reduce its operating costs.

References

Albitar et al., 2013 – *Albitar, H., Ananiev, A., Kalaykov, I.* (2013). New concept of in-water surface cleaning robot. 2013 *IEEE International Conference on Mechatronics and Automation*, Takamatsu. Pp. 1582-1587.

Albitar et al., 2014 – *Albitar, H., Ananiev, A., Kalaykov, I.* (2014). In-water surface cleaning robot: concept, locomotion and stability. *Int J Mechatron Auto* 4(2): 104-115. DOI: https://doi.org/10.1504/ijma.2014.062338

Albitar et al., 2016 – *Albitar, H., Dandan, K., Ananiev, A., Kalaykov, I.* (2016). Underwater robotics: surface cleaning technics, adhesion and locomotion systems. *Int J Adv Robot Syst* 13(1): 7. DOI: https://doi.org/10.5772/62060

Aldrich, Qi, 2005 – *Aldrich, C., Qi B.C.* (2005). Removal of organic foulants from membranes by use of ultrasound. *Water Research Commission. University of Stellenbosch, Stellenbosch WRC Report*. 1229(1): 05.

Asbeck et al., 2006 – *Asbeck, A.T., Kim, S., McClung, A., Parness, A., Cutkosky, M.R.* (2006). Climbing walls with microspines. *IEEE International Conference on Robotics and Automation*, Orlando. Pp. 4315-4317.

Balashov et al., 2011 – *Balashov, V.S, Gromov, BA., Ermolov, I.L., Roskilly, A.P.* (2011). Cleaning by means of the HISMAR autonomous robot. *Russ, Eng, Res*. 31(6): 589-592. DOI: https://doi.org/10.3103/s1068798x11060049

Bax et al., 2003 – *Bax, N., Williamson, A., Aguero, M., Gonzalez, E., Geeves, W.* (2003). Marine invasive alien species: a threat to global biodiversity. *Mar Policy,* 27(4): 313-323. DOI: https://doi.org/10.1016/s0308-597x(03)00041-1

Bixler, Bhushan, 2012 – *Bixler, G., Bhushan, B.* (2012). Review article: Biofouling: Lessons from nature. *Philosophical transactions. Series A, Mathematical, physical, and engineering sciences*. 370: 2381-417. DOI: 10.1098/rsta.2011.0502

Bixler, Bhushan, 2012 – *Bixler, G.D., Bhushan, B.* (2012). Biofouling: lessons from nature. *Philos Trans R Soc A Math Phys Eng Sci.* 370(1967): 2381-2417. DOI: https://doi.org/10.1098/rsta.2011.0502

Caduff, 1990 – *Caduff, E.A.* (1990) Robotic ultrasonic cleaning and spraying device for ships' hulls. U.S. Patent No. 4890567. Washington: U.S. Patent and Trademark Office. Pp. 3-5

Chambers et al., 2006 – *Chambers, L.D., Stokes, K.R., Walsh, F.C., Wood, R.J.* (2006). Modern approaches to marine antifouling coatings. *Surf Coat Technol.* 201(6): 3642-3652. DOI: https://doi.org/10.1016/j.surfcoat.2007.04.001

Chen et al., 2010 – *Chen, G.X., Kwee, T.J., Lei, N.R., Tan, K.P., Choo, Y.S., Hong M.H.* (2010). Underwater laser cleaning for marine and offshore applications. *International Congress on Applications of Lasers & Electro-Optics*, Anaheim, California, USA. Pp. 456-460.

Chen et al., 2012 – *Chen, G.X., Kwee, T.J., Tan, K.P., Choo, Y.S., Hong, M.H.* (2012). High-power fibre laser cleaning for green shipbuilding. *J Laser Micro/Nanoeng.* 7(3): 249-253. DOI: https://doi.org/10.2961/jlmn.2012.03.0003

Chen et al., 2017 – *Chen, R., Fu Q., Liu, Z, Hu, X., Liu, M., Song, R.* (2017). Design and experimental research of an underwater vibration suction module inspired by octopus suckers. *IEEE International Conference on Robotics and Biomimetics (ROBIO)*, Macau. Pp. 1002-1007.

Cioanta, McGhin, 2017 – *Cioanta, I., McGhin, C.* (2017). Cleaning and grooming water submerged structures using acoustic pressure shock waves. U.S. Patent No. 9840313, Washington, DC: U.S. Patent and Trademark Office. Pp. 3-4.

Courson, Shelburne, 2001 – *Courson, B., Shelburne, J.* (2001). Portable encapsulated underwater ultrasonic cleaner. U.S. Patent No. 6259653, Washington, DC: U.S. Patent and Trademark Office. Pp. 1-2.

Daltorio et al., 2005 – *Daltorio, K.A., Horchler, A.D., Gorb, S., Ritzmann, R.E., Quinn, R.D.* (2005). A small wall-walking robot with compliant, adhesive feet. 2005 *IEEE International Conference on Intelligent Robots and Systems*, Edmonton. Pp. 3648-3653.

Davidson et al., 2008 – *Davidson, I.C., McCann, L.D., Sytsma, M.D., Ruiz, G.M.* (2008). Interrupting a multi-species bioinvasion vector: the efficacy of in-water cleaning for removing biofouling on obsolete vessels. *Mar Pollut Bull*. 56(9): 1538-1544. DOI: https://doi.org/10.1016/j.marpolbul.2008.05.024

Drake, Lodge, 2007 – *Drake, J.M., Lodge, D.M.* (2007). Hull fouling is a risk factor for intercontinental species exchange in aquatic ecosystems. *Aquat Invasions*. 2(2): 121-131. DOI: https://doi.org/10.3391/ai.2007.2.2.7

Erneland, 2014 – *Erneland M.B.* (2014). Ultrasonic cleaning of marine geophysical equipment. U.S. Patent Application No. 13/629,412, Washington, DC: U.S. Patent and Trademark Office. Pp. 1-3.

Ferreira et al., 2013 – *Ferreira, C.Z., Conte, G.Y.C., Avila, J.P.J., Pereira, R.C., Ribeiro, T.M.C.* (2013). Underwater robotic vehicle for ship hull inspection: control system architecture. *22nd International Congress of Mechanical Engineering*, Ribeirão Preto, Brazil. Pp. 1231-1241.

Floerl et al., 2010 – *Floerl, O., Peacock, L., Seaward, K., Inglis, G.* (2010). Review of biosecurity and contaminant risks associated with in-water cleaning. The Department of Agriculture, Fisheries and Forestry, Sydney, Australia The National Institute of Water and Atmospheric Research Report.

Fowler, 1987 – *Fowler, M.P.* (1987). Optical cleaning system for removing matter from underwater surfaces. U.S. Patent No. 4689523, Washington, DC: U.S. Patent and Trademark Office. Pp. 2-3.

Godwin, 2003 – *Godwin, L.S.* (2003). Hull fouling of maritime vessels as a pathway for marine species invasions to the Hawaiian Islands. *Biofouling*. 19(S1): 123-131. DOI: https://doi.org/10.1080/0892701031000061750

Holappa et al., 2013 – *Holappa, K.W., Darling, D.T., Hertel III, W.M.* (2013). Robotic submersible cleaning system. U.S. Patent No. 8506719, Washington, DC: U.S. Patent and Trademark Office. Pp. 4-5.

Hopkins et al., 2009 – *Hopkins, G., Forrest, B., Coutts, A.* (2009). Determining the efficacy of incursion response tools: rotating brush technology (coupled with suction capability). MAF Biosecurity, Wellington, New Zealand MAF Biosecurity Technical Report, Research Project ZBS2005-21

Hua et al., 2018 – *Hua, J., Chiu, Y.S., Tsai, C.Y.* (2018). En-route operated hydroblasting system for counteracting biofouling on ship hull. *Ocean Eng*. 152: 249-256. DOI: https://doi.org/10.1016/j.oceaneng.2018.01.050

Huang et al., 2017 – *Huang, Z., Chen, Y., Yang, C., Fan, J., Jiang, P.* (2017). Teleoperate system of underwater cleaning robot based on HUD. *11th Asian Control Conference (ASCC)*, Gold Coast, Australia. Pp. 2675-2679.

Joliot, Joliot, 2005 – *Joliot, P., Joliot, A.* (2005). Quantification of Cyclic and Linear Flows in Plants. *Proc. Natl. Acad. Sci. USA*. 102: 4913-4918.

Kalumuck et al., 1997 – *Kalumuck, K.M., Chahine, G.L., Frederick, G.S., Aley, PD.* (1997). Development of a DYNAJET cavitating water jet cleaning tool for underwater marine fouling removal. *9th American Waterjet Conference*, Dearborn, Michigan, USA. Pp. 541-554.

Kostenko et al., 2019 – *Kostenko, V.V., Bykanova, A.Y., Tolstonogov, A.Y.* (2019). Underwater robotics complex for inspection and laser cleaning of ships from biofouling. *IOP Conf Ser: Earth Environ Sci*. 272(2): 1-7.

Lakretz et al., 2009 – *Lakretz, A., Ron, E.Z., Mamane, H.* (2009). Biofouling control in water by various UVC wavelengths and doses. *Biofouling*. 26(3): 257-267. DOI: https://doi.org/10.1080/08927010903484154

Lazar, Schansker, 2009 – *Lazar, D., Schansker, G.* (2009). Models of chlorophyll *a* fluorescence transient. *Photosynthesis in Silico*, Laisk, A., Nedbal, L., and Govindjee, Eds., Dordrecht: Springer. Pp. 85-123.

Lee et al., 2012 – *Lee, M.H., Park, Y.D., Park, H.G., Park, W.C., Hong, S., Lee, K.S., Chun, H.H.* (2012). Hydrodynamic design of an underwater hull cleaning robot and its evaluation. *Int J Naval Arch Ocean Eng*. 4(4): 335-352. DOI: https://doi.org/10.3744/jnaoe.2012.4.4.335

Legg et al., 2015 – *Legg, M., Yücel, M.K., De Carellan, .IG., Kappatos, V., Selcuk, C., Gan, T.H.* (2015). Acoustic methods for biofouling control: a review. *Ocean Eng*. 103: 237-247. DOI: https://doi.org/10.1016/j.oceaneng.2015.04.070

Lenbaum et al., 2015 – *Lenbaum, V.V., Bulychev, A.A., Matorin, D.N.* (2015). Effects of far-red light on the induction changes of prompt and delayed fluorescence and the redox state of p700 in scenedesmus quadricauda. *Russian Journal of Plant Physiology*. 62(2): 210-218.

Longo, Muscato, 2006 – *Longo, D., Muscato, G.* (2006). The Alicia/sup 3/climbing robot: a three-module robot for automatic wall inspection. *IEEE Robot Autom Mag*. 13(1): 42-50. DOI: https://doi.org/10.1109/mra.2006.1598052

Mazue et al., 2011 – *Mazue, G., Viennet, R., Hihn, J.Y., Carpentier, L., Devidal, P., Albaïna, I.* (2011). Large-scale ultrasonic cleaning system: design of a multi-transducer device for boat cleaning (20 kHz). *Ultrason Sonochem*. 18(4): 895-900. DOI: https://doi.org/10.1016/j.ultsonch.2010.11.021

Menon et al., 2004 – *Menon, C., Murphy, M., Sitti, M.* (2004). Gecko inspired surface climbing robots. 2004 *IEEE International Conference on Robotics and Biomimetics*, Shenyang, China. Pp. 4310436.

Miyake et al., 2005 – *Miyake, C., Miyata, M., Shinzaki, Y., and Tomizawa, K.-I.* (2005). CO_2 Response of Cyclic Electron Flow around PSI (CEF-PSI) in Tobacco Leaves: Relative Electron Fluxes through PSI and PSII Determine the Magnitude of Non-Photochemical Quenching (NPQ) of Chl Fluorescence. *Plant Cell Physiol*. 46: 629-637.

Morrisey, Woods, 2015 – *Morrisey, D.J., Woods, C.* (2015). In-water cleaning technologies: review of information. Publications Logistics Office, Ministry for Primary Industries, Wellington, Pp. 20-25.

Murphy et al., 2006 – *Murphy, M.P, Tso, W., Tanzini, M., Sitti, M.* (2006). Waalbot: an agile smallscale wall climbing robot utilizing pressure sensitive adhesives. 2006 *IEEE/RSJ International Conference on Intelligent Robots and Systems*, Beijing. Pp. 3411-3416.

Nassiraei et al., 2012 – *Nassiraei, A.A.F., Sonoda. T, Ishiim, K.* (2012). Development of ship hull cleaning underwater robot. 2012 *Fifth International Conference on Emerging Trends in Engineering and Technology*, Himeji. Pp. 157-162.

Oliveira, 2017 – *Oliveira, D.* (2017). The enemy below-adhesion and friction of ship hull fouling. Master thesis, Chalmers University of Technology, Gothenburg, Sweden. Pp. 56-67.

Orlova, Rodionov, 2020 – *Orlova, M.I., Rodionov, V.A.* (2020). Biofouling, marine and continental waters: theory, practice, prospects for regional interdisciplinary research. *Fundamental and Applied Hydrophysics*. 13(4): 121-136. DOI: 10.7868/S2073667320040103

Ovchinnikov et al., 1974 – *Ovchinnikov, Yu. A., Ivanov, V.T., Shkrob, A.M.* (1974). Membranoaktivnye kompleksony [Membrane Active Complexones]. Moscow: Nauka. 64 p. [in Russian]

Schansker et al., 2003 – *Schansker, G., Srivastava, A., Strasser, R.J.*, and Govindjee (2003). Characterization of the 820-nm transmission signal paralleling the chlorophyll *a* fluorescence rise (OJIP) in pea leaves. *Funct. Plant Biol*. 30: 785-796.

Schansker et al., 2005 – *Schansker, G., Toth, S.Z., Strasser, R.J.* (2005). Methylviologen and dibromothymoquinone treatments of pea leaves reveal the role of photosystem I in the Chl *a* fluorescence rise OJIP. *Biochim. Biophys. Acta*. 1706: 250-261.

Zvyagintsev, 2005 – *Zvyagintsev, A.Yu.* (2005). Marine fouling in the northwestern part of the Pacific Ocean. Vladivostok: Dalnauka. 432 p.

Zvyagintsev, Moshchenko, 2002 – *Zvyagintsev, A.Yu., Moshchenko, A.V.* (2002). The role of microscale turbulence in the distribution of macrofouling organisms on the hulls of long-distance ships. *Biology of the sea*. 6: 449-453.

Published in the USA
Biogeosystem Technique
Issued since 2014.
E-ISSN: 2413-7316
2024. 11(2): 124-129

DOI: 10.13187/bgt.2024.2.124
https://bgt.cherkasgu.press

Influence of Homocysteine on Metabolic Processes in Biological Systems

Rufiya G. Karimova [a, *], Anna N. Lebedeva [a], Ekaterina A. Gorokhova [a]

[a] Kazan (Volga Region) Federal University, Kazan, Russian Federation

Paper Review Summary:
Received: 2024, October 21
Received in revised form: 2024, December 11
Acceptance: 2024, December 26

Abstract

The study is devoted to determining the level of homocysteine in mammals and determining the extent of its influence on metabolic processes.

Homocysteine is a sulfur-containing non-proteinogenic amino acid that is formed as a result of the oxidation-reduction metabolism of methionine. Homocysteine metabolism includes transmethylation, remethylation, and transsulfation reactions. When metabolism is disrupted, homocysteine formation increases, which leads to hyperhomocysteinemia.

In this work, homocysteine levels were determined in rats with experimental heart failure and experimental chronic kidney disease in rats. Chronic heart failure was modeled by intraperitoneal administration of phenylephrine for 28 days. Chronic kidney disease was modeled by 5/6 nephrectomy. The residual kidney resection model was performed in two sessions under 2 % isoflurane anesthesia: during the first week, approximately 2/3 of the left kidney was removed from the rats, and during the second week, the entire right kidney was removed. The level of homocysteine, creatinine, urea, potassium, sodium, chlorine ions, aspartate aminotransferase, alanine aminotransferase, lactate dehydrogenase activity were determined in the blood 2 and 6 months after pathology modeling.

Based on the results of the studies, it was established that an increase in homocysteine levels is observed in a number of pathologies, such as chronic heart failure and chronic kidney disease. An increase in the concentration of homocysteine in the blood plasma was revealed as the pathology progressed. The level of homocysteine in plasma correlates with the level of creatinine and urea and is absolutely not associated with the level of sodium, potassium, chloride ions and the activity of metabolic enzymes. The results of the study allow us to recommend measuring the concentration of homocysteine in plasma to determine the degree of metabolic disorders.

Keywords: homocysteine, blood, metabolites, creatinine, urea, heart, kidneys, biological systems, enzymes, ions.

1. Introduction

Homocysteine (Hcy) is a sulfur-containing non-proteinogenic amino acid that is formed as a result of the redox metabolism of methionine. Hcy metabolism involves transmethylation,

* Corresponding author
E-mail addresses: Rufiya77@yandex.ru (R.G. Karimova)

remethylation, and transsulfation reactions. In most cells, through the transmethylation of Hcy in the methionine metabolic cycle, the methyl group of activated methionine (S-adenosylmethionine or SAM) is attached to methyl acceptors (DNA, RNA, and protein) by methyltransferases, and S-adenosyl-Hcy (SAH) is rapidly hydrolyzed to adenosine and Hcy, resulting in hyperhomocysteinemia. Once formed, Hcy can be recycled to methionine or converted to cysteine by remethylation and transsulfation, respectively. Hcy is remethylated to methionine through two separate reactions catalyzed by three different enzymes. In all tissues, folate donates a methyl group via methylenetetrahydrofolate reductase (MTHFR) in a reaction catalyzed by methionine synthase, a vitamin B12-dependent enzyme (Esse et al., 2019). Otherwise, mainly in the mammalian heart, liver, and kidney, Hcy is remethylated using betaine, which donates a methyl group by betaine-Hcy S-methyltransferase (BHMT). Betaine is found in some foods such as wheat germ or bran, spinach, beets, seafood, and legumes. Studies have confirmed the ability of betaine to reduce Hcy levels in the presence of excess methionine intake, and the fact that low-dose betaine supplementation results in immediate and long-term reductions in plasma Hcy levels in healthy individuals (Steenge et al., 2003, Olthof et al., 2003). The remethylation process begins at low concentrations of Hcy and methionine (McRae, 2013). On the other hand, mainly in the liver, but also in the kidneys, small intestine and pancreas (Zaric et al., 2019), Hcy is enzymatically modified by cystathionine β-synthase, a vitamin B6-dependent enzyme, to irreversibly form cysteine via the intermediate cystathionine. The transsulfuration pathway results in the formation of sulfur metabolites including GSH, a key cellular antioxidant, and hydrogen sulfide (H_2S), which acts as a gaseous signaling molecule. The transsulfuration pathway becomes active when Hcy and methionine concentrations increase (Verhoef et al., 2005).

In plants, Hcy is synthesized by two pathways. One involves the plastid/chloroplast and involves a pathway from sulfate via the formation of cysteine and cystathionine (CysT); however, next to cysteine, also O-phosphohomoserine can be metabolized to CysT by CysT γ-synthase. β-cleavage of CysT to Hcy is catalyzed by cystathionine β-lyase (CBL) (Ravanel et al., 2005). The other cytosolic pathway involves the formation of Hcy as a by-product of the methylation reaction in plant cells (Jakubowski, 2006). In this regard, S-adenosylhomocysteine (AdoHcy) is converted to Hcy in a reaction catalyzed by S-adenosylhomocysteine hydrolase (SAHH) (Ravanel et al., 2005).

Most studies confirm an increase in homocysteine levels in various pathologies, but data on the correlation of homocysteine levels with metabolic parameters remain unstudied.

The aim of our research was to study the correlation of homocysteine levels with metabolic parameters of the blood in experimental chronic failure and chronic renal disease in rats.

2. Methodology

Modeling of chronic heart failure (CHF) and chronic kidney disease was performed on male Wistar rats. All experimental protocols complied with international ethical standards for the humane treatment of animals and were approved by the Local Ethics Committee of KFU (protocol 33 dated 11/25/2021). The animals were housed according to the guidelines for animal research, with constant room temperature, a 12-hour light/dark cycle, and 50±5 % humidity, as well as standard chow and water ad libitum.

The animals were divided into 3 groups:

1. Control (n = 16)
2. Rats with experimental chronic heart failure (n = 16)
3. Rats with experimental chronic kidney disease (n = 16).

Chronic heart failure was modeled by intraperitoneal administration of phenylephrine for 28 days (Rajanathan et al., 2022).

Chronic kidney disease was modeled by 5/6 nephrectomy. The residual kidney resection model was performed in two sessions under 2 % isoflurane anesthesia: in the first week, approximately 2/3 of the left kidney was removed from the rats, and in the second week, the entire right kidney was removed. After surgery, the rats were given free access to tap water and standard rat chow (Nishiyama et al., 2019).

The level of homocysteine, creatinine, urea, potassium, sodium, chlorine ions, aspartate aminotransferase, alanine aminotransferase, lactate dehydrogenase activity were measured in the blood 2 and 6 months after pathology modeling. The level of homocysteine was determined in blood plasma by a colorimetric method on a Thermo Scientific Multiskan F analyzer using a kit from Elabscience Biotechnology Co., Ltd. Biochemical analysis of blood plasma was performed by photometric method using commercial kits.

To test the normal distribution of data, Fisher's F-test and Shapiro-Wilk test were used using OriginPro 8.5 software. To compare two independent groups and paired data, Mann-Whitney U-test and Wilcoxon paired test were used, respectively. Correlation analysis was performed using Pearson coefficient.

3. Results and discussion

After modeling heart failure, rats developed cardiomegaly (Figure 1).

Fig. 1. Lateral radiograph of a rat with left-sided chronic heart failure. Severe cardiomegaly, especially in the left atrium

The studies showed that the level of homocysteine in the blood plasma gradually increased with the development of chronic heart failure.

In healthy rats of the control group, the level of homocysteine in the blood was 6.75 ± 0.25 µmol/l. Immediately after the end of the modeling, the level of homocysteine did not change, while clinical symptoms of heart failure were pronounced.

Two months after the modeling of heart failure, the level of homocysteine increased to 14.9 ± 0.66 µmol/l, and after 6 months to 21.5 ± 0.7 µmol/l (Figure 2).

This fact calls into question the claims of many authors that hyperhomocysteinemia is a risk factor for cardiovascular diseases (Jakubowski, 2019; Kim et al., 2018; Kubota et al., 2019). Our data confirm the studies of Wang X et al. (2023), who found no causal relationship between elevated plasma homocysteine levels and cardiovascular diseases.

At the same time, the study of metabolic parameters showed that the level of homocysteine correlated with the level of creatinine in the blood, which also increased as chronic heart failure developed. The remaining parameters studied were independent of the level of plasma homocysteine (Table 1).

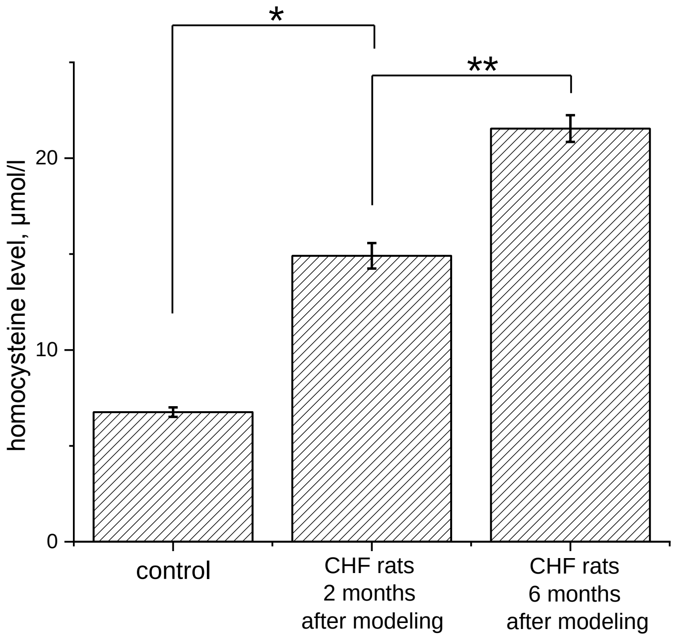

Fig. 2. Homocysteine levels in rats with experimental chronic heart failure,
*– is the significance of differences p≤0.05

Table 1. Changes in the biochemical composition of blood in rats with CHF

Parameter	Control	CHF rats 2 months after modeling	CHF rats 6 months after modeling
Urea, mmol/l	6.8±0.7	8.4±0.71*	8.3±0.71
Creatinine, μmol/l	71.6±8.2	136.1±18.4*	158.6±19.0*
AST, U/l	20.6±2.07	40.2±3.5	77.5±6.5*
ALT, U/l	40.6±2.62	38.6±2.9	40.2±2.9
LDH, U/l	21.7±1.19	29.8±3.9	31.7±6.9
Na, mmol/l	156.3±3.06	148.5±0.92	152.4±0.92
K, mmol/l	4.15±0.94	3.69±0.48	3.89±0.48
Cl, mmol/l	90.5±4.5	86.2±5.28	99.2±1.28

*– is the significance of differences p≤0.05

Experimental chronic kidney disease was also accompanied by an increase in the level of homocysteine in the blood. In experimental chronic kidney disease, it is higher than in chronic heart failure. Two months after modeling, the concentration of homocysteine in the blood plasma is 17.46±0.57 μmol/l, and after 4 months it increases to 30.25±0.68 μmol/l (Figure 3). A positive correlation with the level of creatinine and urea in the blood was revealed (Table 2).

Therefore, the level of homocysteine increases with the progression of renal pathology and can be used as a marker for predicting the development of the severity of renal failure.

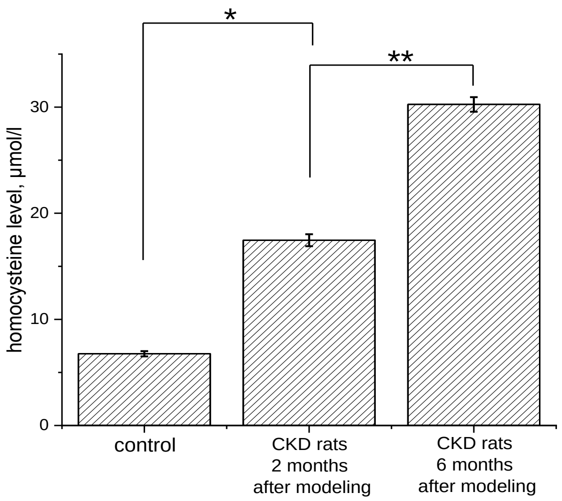

Fig. 3. Homocysteine levels in rats with experimental chronic kidney disease,
* – is the significance of differences p≤0.05

Table 2. Changes in the biochemical composition of blood in rats with CKD

Parameter	Control	CHF rats 2 months after modeling	CHF rats 6 months after modeling
Urea, mmol/l	6.8±0.7	36.8±2.7*	53±2.7*
Creatinine, µmol/l	71.6±8.2	186±9.4*	221±9.4*
AST, U/l	20.6±2.07	20.8±2.47	22±2.47
ALT, U/l	40.6±2.62	42.6±2.82	48±2.82
Na, mmol/l	156.3±3.06	162.5±3.06	170±3.06
K, mmol/l	4.15±0.94	3.65±0.94	3.15±0.94
Cl, mmol/l	90.5±4.5	85.4±4.5	79±4.5

*– is the significance of differences p≤0.05

There is sufficiently strong clinical evidence that hyperhomocysteinemia does not cause renal failure (Samuelsson et al., 1999; Sarnak et al., 2002; Hovind et al., 2001), although a recent study has linked higher homocysteine levels with a greater decrease in glomerular filtration rate (Ninomiya et al., 2004). Therefore, the association between hyperhomocysteinemia and renal dysfunction may be causal, i.e. renal failure causes elevated plasma homocysteine levels, but this association may also be due to other co-factors that, on the one hand, lead to renal dysfunction and, on the other hand, cause hyperhomocysteinemia through different mechanisms. Evidence for the association between hyperhomocysteinemia and the progression of chronic renal failure is the lack of a significant relationship between enzyme activity (aspartate aminotransferase, alanine aminotransferase) and the concentration of plasma ions in the blood (sodium, potassium, chloride ions).

4. Conclusion and recommendations

An increase in the homocysteine level in biological systems is an indicator of metabolic disorders. The concentration of homocysteine in the blood plasma of mammals positively correlates with the final metabolites of blood plasma, which allows it to be used to predict the development of a number of pathologies, including chronic heart failure and chronic renal disease.

5. Funding

The work was supported by the Russian Science Foundation, project 23-26-00167.

References

Esse et al., 2019 – *Esse, R., Barroso, M., Almeida, I., Castro, R.* (2019). The contribution of homocysteine metabolism disruption to endothelial dysfunction: State-of-the-art. *Int. J. Mol. Sci.* 20, 867. DOI: 10.3390/ijms20040867

Hovind et al., 2001 – *Hovind, P., Tarnow, L., Rossing, P.* (2001). Progression of diabetic nephropathy: role of plasma homocysteine and plasminogen activator inhibitor-1. *Am. J. Kidney Dis*. 38: 1376-1380 DOI: 10.1053/ajkd.2001.29261

Jakubowski, 2006 – *Jakubowski, H.* (2006). Pathophysiological consequences of homocysteine excess. *J. Nutr*. 136: 1741S-1749S. DOI: 10.1093/jn/136.6.1741S

Jakubowski, 2019 – *Jakubowski, H.* (2019). Homocysteine modification in protein structure/function and human disease. *Physiol Rev*. 99: 555-604. DOI: 10.1152/physrev.00003.2018

Kim et al., 2018 – *Kim, J., Lee, S., Yoon, D., Shin, C.* (2018). Concurrent presence of obstructive sleep apnea and elevated homocysteine levels exacerbate the development of hypertension: a KoGES six-year follow-up study. *Sci Rep*. 8: 2665. DOI: 10.1038/s41598-018-21033-5

Kubota et al., 2019 – *Kubota, Y, Alonso, A., Heckbert, S., Norby, F., Folsom, A.* (2019). Homocysteine and incident atrial fibrillation: the atherosclerosis risk in communities study and the multi-ethnic study of atherosclerosis. *Heart Lung Circulat*. 28: 615-22. DOI: 10.1016/j.hlc.2018.03.007

McRae, 2013 – *McRae, M.P.* (2013). Betaine supplementation decreases plasma homocysteine in healthy adult participants: A meta-analysis. *J. Chiropr. Med*. 12: 20-25. DOI: 10.1016/j.jcm.2012.11.001

Ninomiya et al., 2004 – *Ninomiya, T., Kiyohara, Y., Kubo, M.* (2004). Hyperhomocysteinemia and the development of chronic kidney disease in a general population: the Hisayama study. *Am. J. Kidney Dis*. 44: 437-445

Nishiyama et al., 2019 – *Nishiyama, K., Aono, K., Fujimoto, Y., Kuwamura, M., Okada, T., Tokumoto, H., Izawa, T., Okano, R., Nakajima, H., Takeuchi, T., Azuma, Y.T.* (2019). Chronic kidney disease after 5/6 nephrectomy disturbs the intestinal microbiota and alters intestinal motility. *J. Cell Physiol*. 234(5): 6667-6678. DOI: 10.1002/jcp.27408

Olthof et al., 2003 – *Olthof, M.R., van Vliet, T., Boelsma, E., Verhoef, P.* (2003). Low dose betaine supplementation leads to immediate and long term lowering of plasma homocysteine in healthy men and women. *J. Nutr*. 133: 4135-4138. DOI: 10.1093/jn/133.12.4135

Rajanathan et al., 2022 – *Rajanathan, R, Pedersen, T.M., Thomsen, M.B., Botker, H.E., Matchkov, V.V.* (2022). Phenylephrine-Induced Cardiovascular Changes in the Anesthetized Mouse: An Integrated Assessment of *in vivo* Hemodynamics Under Conditions of Controlled Heart Rate. *Front Physiol*. 13: 831724. DOI: 10.3389/fphys.2022.831724

Ravanel et al., 2005 – *Ravanel, S., Job, D., Douce, R.* (1996). Purification and properties of cystathionine beta-lyase from Arabidopsis thaliana overexpressed in Escherichia coli. *Biochem J*. 1,320 (Pt 2): 383-392. DOI: 10.1042/bj3200383

Samuelsson et al., 1999 – *Samuelsson, O., Lee, D.M., Attman, P.O.* (1999). The plasma levels of homocysteine are elevated in moderate renal insufficiency but do not predict the rate of progression. *Nephron*. 82: 306-311. DOI: 10.1159/000045445

Sarnak et al., 2002 – *Sarnak, M.J., Wang, S.R., Beck, G.J.* (2002). Homocysteine, cysteine, and B vitamins as predictors of kidney disease progression. *Am. J. Kidney* 40: 932-939. DOI: 10.1053/ajkd.2002.36323

Steenge et al., 2003 – *Steenge, G.R., Verhoef, P., Katan, M.B.* (2003). Betaine supplementation lowers plasma HCY in healthy men and women. *J. Nutr*. 133: 1291-1295. DOI: 10.1093/jn/133.5.1291

Verhoef et al., 2005 – *Verhoef, P., van Vliet, T., Olthof, M.R., Katan, M.B.* (2005). A high-protein diet increases postprandial but not fasting plasma total homocysteine concentrations: A dietary controlled, crossover trial in healthy volunteers. *Am. J. Clin. Nutr*. 82: 553-558. DOI: 10.1093/ajcn.82.3.553

Wang et al., 2023 – *Wang, X., Chen, Z., Tian, W., Zhang, J., Li, Q., Ju, J., Xu, H., Chen, K.* (2023). Plasma homocysteine levels and risk of congestive heart failure or cardiomyopathy: A Mendelian randomization study. *Front Cardiovasc Med*. 10: 1030257. DOI: 10.3389/fcvm.2023.1030257

Zaric et al., 2019 – *Zaric, L.B., Obradovic, M., Bajic, V., Haidara, M.A., Jovanovic, M., Isenovic, E.R.* (2019). Homocysteine and Hyperhomocysteinaemia. *Curr. Med. Chem*. 26: 2948-2961. DOI: 10.2174/0929867325666180313105949

Published in the USA
Biogeosystem Technique
Issued since 2014.
E-ISSN: 2413-7316
2024. 11(2): 130-131

DOI: 10.13187/bgt.2024.2.130
https://bgt.cherkasgu.press

In Memoriam

In Memoriam of Valery Ivanovich Glazko

Valery P. Kalinitchenko [a, *]

[a] Institute of Soil Fertility of South Russia, Persianovsky, Russian Federation

In memoriam of Valery Ivanovich Glazko passed away on July 30, 2024, at the 76th year of life. Doctor of Agricultural Sciences, Academician of the Russian Academy of Sciences, Academician and member of the Presidium of the Russian Academy of Natural Sciences, Member of the Nanotechnology Society of Russia, Laureate of the Government of the Russian Federation in the field of education.

Fig. 1. Valery Ivanovich Glazko

* Corresponding author
E-mail addresses: kalinitch@mail.ru (V.P. Kalinitchenko)

Valery Ivanovich Glazko was a member of the Editorial Board of the journal Biogeosystem Technique. He made a great contribution in formulation the journal's objective and defined the publication policy. Based on a genetics systematic, his series of articles in the journal on the genomics, biotechnology and ecology potential opened up the new solutions to the genetics and environmental protection fundamental problems.

His research in the field of evolutionary, population and ecological genetics, the genetic foundations of speciation and domestication, biotechnology, the use of DNA technologies in agriculture, the coevolution of human and domesticated animal gene pools allowed him to formulate a number of important hypotheses and concepts of agroecobiocenoses sustainable development, genetic diversity conservation, and opened the domestication mechanisms.

Valery Ivanovich Glazko is an outstanding Russian scientist, geneticist, radiation biologist, biotechnologist and molecular biologist. He was the author of 1,000 scientific papers.

He was a member of the editorial boards of many influential scientific journals.

He was born on January 30, 1949 in the city of Leninogorsk, Kazakh SSR. In 1972, he graduated from the Faculty of Natural Sciences of Novosibirsk State University with a degree in genetics. Doctor of Sciences since 1991.

Valery Ivanovich will remain in our memory as an example of a thinker, a bearer of deep fundamental knowledge, decency, and kindness, presenting a bright image of a Russian scientist.